The Canadian Mineralogist
Vol. 41, pp. 1203-1224 (2003)

CRYSTAL CHEMISTRY OF THE ROSENBUSCHITE GROUP

CLAES C. CHRISTIANSEN[§] AND OLE JOHNSEN

Geological Museum, University of Copenhagen, Øster Voldgade 5-7, DK-1350 Copenhagen K, Denmark

EMIL MAKOVICKY

Geological Institute, University of Copenhagen, Øster Voldgade 10, DK-1350 Copenhagen K, Denmark

ABSTRACT

The minerals of the rosenbuschite group are sorosilicates composed of a framework of 6- to 8-corner polyhedra and rows of Si_2O_7 dimers. The polyhedra combine into layers (*O* layers) and into ribbons by edge sharing. Heterogeneous layers (*H* layers), composed of the octahedra from the ribbons and the sorosilicate groups, alternate with the *O* layer into a layered *HOH* structure. The 6- to 8-corner polyhedra host a variety of cations: Na, Mg, Ca, Ti, Mn, Fe, Y, Zr, Nb and the REE. Substitutions among these elements affect the geometrical properties of the various polyhedra. Crystal-structure refinements (X-ray diffraction) have been done on five specimens of the rosenbuschite group: götzenite, hainite, kochite (a new member of the group), rosenbuschite and seidozerite. Detailed models for their site occupancies are derived by fitting scattering values of the sites to the chemical composition, and the weighted bond-valence sums to valence sums in an integrated calculation procedure. Results of chemical analyses suggest a series of intermediate compositions between götzenite and kochite. This series may be described as a solid-solution series in which Zr substitutes for Ca in one structural position, götzenite being the Ca-rich end-member. Through substitution of Ti by Zr, still another solid-solution exists between kochite and rosenbuschite, with rosenbuschite as the Zr-rich member. The Ca → Zr substitution has significant effect on the size of the respective octahedron, as well as on the dimension and distortion of the adjacent polyhedra. The reduction in size of the Ca → Zr octahedron is partly compensated by an enlargement of the dimensions of the adjacent Ti octahedron. This change favors the Ti → Zr substitution at the latter site. Different degrees of distortion in the sorosilicate group and the adjacent Ca, Na octahedra are also associated with the Ca → Zr substitution. In the Zr-rich seidozerite, a stacking of the *HOH* structural layers different from the above-mentioned structures is observed. The change in stacking sequence is closely related to complex geometrical interrelationships between dimensions and distortions of the Zr- and Mn-dominated octahedra. Chemical data indicate that seidozerite does not form a solid solution with rosenbuschite.

Keywords: rosenbuschite group, seidozerite, crystal chemistry, single-crystal X-ray diffraction, electron-microprobe data, cation order, polyhedron geometry.

SOMMAIRE

Les minéraux du groupe de la rosenbuschite sont des sorosilicates dont la trame est composée de polyèdres à de six à huit coins et des rangées de dimères Si_2O_7. Les polyèdres sont agencés en couches (niveaux *O*) et en rubans par partage d'arêtes. Les couches hétérogènes (niveaux *H*), composée d'octaèdres des rubans et de groupes sorosilicatés, alternent avec les niveaux *O* pour former une structure stratifiée *HOH*. Les polyèdres à de six à huit coins renferment une variété de cations: Na, Mg, Ca, Ti, Mn, Fe, Y, Zr, Nb et les terres rares. Les substitutions impliquant ces éléments affectent les propriétés géométriques des divers polyèdres. Nous avons effectué par diffraction X un affinement de la structure de cinq échantillons du groupe de la rosenbuschite: götzenite, hainite, kochite (un nouveau membre du groupe), rosenbuschite et seidozerite. Nous avons dérivé des modèles détaillés de la répartition des cations sur les sites en ajustant les valeurs de la dispersion des rayons X à ces sites avec la composition chimique, et les sommes pondérées des valences de liaison prédites aux valeurs observées, dans le contexte d'une procédure de calcul intégrée. Les compositions déterminées par analyse semblent indiquer une série de membres intermédiaires entre götzenite et kochite. On peur décrire cette série en termes d'une solution solide dans laquelle le Zr remplace le Ca à une position structurale, la götzenite étant le pôle calcique. Grâce à la substitution de Zr au Ti, une autre solution solide existe entre kochite et rosenbuschite, cette dernière étant le pôle zirconifère. La substitution Ca → Zr exerce un effet important sur la dimension des octaèdres respectifs, de même que sur la dimension et la distorsion des polyèdres adjacents. La réduction de la taille de l'octaèdre Ca → Zr serait en partie compensée par une augmentation de la taille des octaèdres adjacents contenant le Ti. Ce changement favorise la substitution Ti → Zr à ce site. Des degrés différents de distorsion du groupe sorosilicaté et des octaèdres adjacents contenant le Ca et le

§ *E-mail address*: claesc@savik.geomus.ku.dk

Na sont aussi associés à la substitution Ca → Zr. La seidozerite, riche en Zr, montre un empilement des séquences stratifiées *HOH* différent de celui des structures mentionnées ci-haut. Ce changement est étroitement lié aux interrelations géométriques complexes entre dimensions et distorsions des octaèdres à dominance de Zr et de Mn. Les données chimiques indiquent que la seidozerite ne forme pas de solution solide avec la rosenbuschite.

(Traduit par la Rédaction)

Mots-clés: groupe de la rosenbuschite, seidozerite, cristallochimie, diffraction X sur monocristal, données à la microsonde électronique, degré d'ordre des cations, géométrie des polyèdres.

Introduction

The rosenbuschite group of minerals are Ca- and Na-containing zirconium and titanium silicates occurring mainly as accessory phases in Si-undersaturated alkaline and in calc-alkaline rocks. They are sorosilicates composed of a framework of corner- and edge-sharing polyhedra and rows of Si_2O_7 groups. The polyhedra containing the 6- to 8-coordinated cations combine into layers (*O* layers) and into ribbons by edge sharing. Heterogeneous layers (*H* layers), composed of the octahedra from the ribbons and the sorosilicate groups, alternate with the *O* layer into a layered *HOH* structure. The minerals contain a wide variety of elements, Na, Mg, Ca, Ti, Mn, Fe, Y, Zr, Nb and the rare-earth elements (REE), which are distributed over the 6- to 8-coordinated cation positions.

We have chemically analyzed a series of rosenbuschite-group minerals from the localities of Werner Bjerge, East Greenland (sample WBC–12 and WBC–13) and Langesund Fjord, Norway (sample LF–A2 and LF–A5). Included in the study also is seidozerite from the Lovozero Complex, Kola Peninsula in Russia (sample 1993.158 from the collection of the Geological Museum of Copenhagen). During the study, doubt arose on the definition of the mineral rosenbuschite, and the type material (sample no. TYROS) described by Brögger (1889) was subsequently included in this work (kindly provided to us by Dan Holtstam from the Museum of Natural History in Stockholm, collection number #531136). We established the chemical compositions of all specimens using an electron microprobe. On that basis, five specimens were chosen for further investigation by means of single-crystal X-ray diffraction.

We offer a detailed description of the cation distribution within the rosenbuschite group and detailed crystal-chemical comparisons of the specimens investigated. We intend to describe and explain the crystal-chemical implications of the substitutions taking place within the group. We concentrate on geometrical properties of the individual coordination polyhedra, set in relation to the overall topology and the cation distribution within each specimen. This approach enables us to provide qualitative arguments concerning the degree of solid solution among the members of the group. Furthermore, seidozerite is introduced as a member of the rosenbuschite group by describing its polytypic relationship to the other members of the group. Finally, we relate the existence of the two configurational polytypes to their different chemical compositions.

Background Information

The group, named after the mineral rosenbuschite, was first described by Brögger in 1887. Thereafter, a number of minerals were suggested to be related to rosenbuschite (Brögger 1889, 1890, Blumrich 1893, Zachariasen 1930, Peacock 1937, Neumann 1962, Sahama *et al.* 1966). It was not until the structure solutions of seidozerite (Simonov & Belov 1960, Skszat & Simonov 1966) and rosenbuschite (Shibaeva *et al.* 1964) that the group could be defined on a structural basis. At present, the group comprises the minerals götzenite (Sahama & Hytönen 1957, Cannillo *et al.* 1972), hainite (Blumrich 1893, Johan & Čech 1989, Rastsvetaeva *et al.* 1995, Atencio *et al.* 1999), rosenbuschite (Brögger 1890) and a new phase, kochite (Christiansen *et al.* 2003), which was discovered in relation to the present work. We include seidozerite (Semenov *et al.* 1958) as a member of the rosenbuschite group because its crystal structure is polytypically related to the minerals of this group (Egorov-Tismenko & Sokolova 1990, Christiansen *et al.* 1999), and the elements contained in seidozerite are also major components in other members of the group. The polytypic layer is the so-called HOH layer characteristic for the plesiotypic family of heterophyllosilicates (Ferraris *et al.* 1996, Ferraris 1997, Christiansen *et al.* 1999). Bafertisite, perraultite, lamprophyllite, and delindeite are all sorosilicate members of this series that have a plesiotypic (Makovicky 1997) relationship to the members of the rosenbuschite group in that the coordination of certain elements differs. The minerals dealt with in this work all have the same coordination of atoms in corresponding positions.

Recently, rosenbuschite-group minerals from different environments have been analyzed by Bulakh & Kapustin (1973), Cundari & Ferguson (1994), Sharygin *et al.* (1996), Atencio *et al.* (1999) and Men'shikov *et al.* (1999). It has become apparent to us that the group has a wide chemical variation with respect to the elements hosted within the framework of octahedra. Especially important in this aspect is the replacement of Ca by Zr in one atomic position. Cannillo *et al.* (1972)

raised the question of an isomorphous series, with götzenite and seidozerite as the two end-members. These two minerals represent the Zr-poor and Zr-rich members of the group, respectively, and rosenbuschite would be an intermediate member. A less extensive series between götzenite and rosenbuschite, with hainite as an intermediate member, has also been suggested by Johan & Čech (1989). Substitution schemes for such series have been worked out purely on the basis of chemical composition and charge considerations (Johan & Čech 1989, Cundari & Ferguson 1994, Sharygin *et al.* 1996). However, a replacement of Ca by Zr does not only affect charge balance but, owing to the quite different ionic radii of the two elements, also causes a reduction in the size of the coordination octahedron. This reduction will affect the geometry of the surrounding coordination polyhedra. However, no analysis of these aspects has yet been conducted.

The general formula $(M1)_4(M2)_4(M3)_4(M4)_2(M5)_2(Si_2O_7)_4F_4X_4$ (M = Na, Mg, Ca, Ti, Mn, Fe, Y, Zr, Nb, and the rare-earth elements, REE, and X = O, F) may be taken to represent all members of the rosenbuschite group. Taking into consideration cation ordering at the M positions and the topological variants in the group, we will show that the simplified chemical formulae of the five members may be given as: götzenite $Ca_2(Ca,Na)_2Ca_2NaTi(Si_2O_7)_2F_2F_2$, hainite $(Ca,Zr,Y)_2(Na,Ca)_2Ca_2NaTi(Si_2O_7)_2F_2F_2$, kochite $Zr_2(Mn,Zr)_2(Na,Ca)_4Ca_4Na_2Ti_2(Si_2O_7)_4F_4O_4$, rosenbuschite $Zr_2Ca_2(Na,Ca)_4Ca_4Na_2ZrTi(Si_2O_7)_4F_4O_4$, and seidozerite $Zr_4Na_2Mn_2Na_4Na_2Ti_2(Si_2O_7)_4F_4O_4$.

Experimental Work

Chemical analyses were conducted on a JEOL 733 electron microprobe using Tracor Northern 5500 and 5600 automation in wavelength-dispersion mode. The electron beam was accelerated over 20 kV with a beam current of 20 nA and had a diameter of 20 μm. Data reduction was performed using a PAP routine in XMAQNT (C. Davidson, CSIRO, pers. commun.). The following standards were used: vlasovite (Zr$L\alpha$), tephroite (Mn$K\alpha$), albite (Na$K\alpha$), diopside (Mg$K\alpha$), almandine (Si$K\alpha$, Fe$K\alpha$), $MnNb_2O_6$ (Nb$L\alpha$), rutile (Ti$K\alpha$), celestine (Sr$L\alpha$), apatite (P$K\alpha$), $TbPO_4$ (Tb$L\alpha$), sanbornite (Ba$L\alpha$), YIG (Y$L\alpha$), $GdPO_4$ (Gd$L\alpha$), hafnon (Hf$M\alpha$), $LaPO_4$ (La$L\alpha$), $CoWO_4$ (W$M\alpha$), $EuPO_4$ (Eu$L\alpha$), chrysoberyl (Al$K\alpha$), $NiTa_2O_6$ (Ta$M\alpha$), $CePO_4$ (Ca$L\alpha$), $SmPO_4$ (Sm$L\alpha$), zincite (Zn$L\alpha$), rubidium-substituted microcline (Ru$L\alpha$), $NdPO_4$ (Nd$L\alpha$), VPO_4 (V$K\alpha$), phlogopite (F$K\alpha$), pollucite (Cs$L\alpha$), $PrPO_4$ (Pr$L\alpha$), $ErPO_4$ (Er$L\alpha$), REE-bearing glass (Sc$K\alpha$), $TmPO_4$ (Tm$L\alpha$), cassiterite (Sn$L\alpha$), $DyPO_4$ (Dy$L\alpha$), $YbPO_4$ (Yb$L\alpha$), sanidine (K$K\alpha$). Empirical formulae were calculated on the basis of eight atoms of Si in agreement with the structure refinements, which invariably show fully occupied silicon positions. Chemical data for the selected specimens are given in Table 1.

TABLE 1. CHEMICAL COMPOSITIONS AND FORMULA UNITS OF MEMBERS OF THE ROSENBUSCHITE GROUP

Sample	WBC-13		WBC-12		LF-A2		LF-A5		TYROS		1993.158	
Mineral	Götzenite		Kochite		Hainite		Rosenbuschite		Rosenbuschite		Seidozerite	
	wt.%	*apfu**	wt.%	*apfu*	wt.%	*apfu*	wt.%	*apfu*	wt.%	*apfu*	wt.%	*apfu*
SiO_2	30.85	8.00	31.19	8.00	30.50	8.00	29.94	8.00	30.51	8.00	30.73	8.00
Al_2O_3	0.05	0.02	0.05	0.02	0.05	0.02	n.d.		n.d.		0.08	0.02
TiO_2	9.24	1.80	8.42	1.62	8.16	1.61	4.56	0.92	6.83	1.35	13.88	2.72
SnO_2	n.d.**		n.d.		n.d.		0.19	0.02	n.d.		n.d.	
ZrO_2	1.41	0.18	11.90	1.49	3.96	0.51	19.66	2.56	15.86	2.03	21.83	2.77
HfO_2	n.d.		0.09	0.01	0.08	0.01	0.46	0.04	0.34	0.03	0.38	0.03
Nb_2O_5	1.12	0.13	1.85	0.21	1.23	0.15	1.35	0.16	2.25	0.27	0.77	0.09
Ta_2O_5	n.d.		0.02	0.00	0.03	0.00	0.11	0.01	0.06	0.00	0.01	0.00
MgO	n.d.		0.01	0.00	n.d.		0.06	0.02	n.d.		1.53	0.59
MnO	1.04	0.23	4.92	1.07	0.73	0.16	0.91	0.21	1.08	0.24	3.86	0.85
FeO	0.44	0.10	1.08	0.23	0.69	0.15	0.50	0.11	0.28	0.06	2.93	0.64
CaO	36.70	10.20	21.39	5.88	29.64	8.33	23.40	6.70	24.54	6.89	1.86	0.52
SrO	0.18	0.03	0.12	0.02	0.08	0.01	0.14	0.02	0.10	0.02	0.19	0.03
Na_2O	6.31	3.17	9.85	4.90	7.45	3.79	9.16	4.75	9.47	4.81	14.69	7.41
Y_2O_3	0.90	0.12	0.38	0.05	4.35	0.61	1.00	0.14	1.28	0.18	0.19	0.03
La_2O_3	1.66	0.16	0.24	0.02	0.63	0.06	n.d.		n.d.		n.d.	
Ce_2O_3	2.71	0.26	0.57	0.05	1.67	0.16	0.13	0.01	0.17	0.02	n.d.	
Nd_2O_3	0.44	0.04	n.d.		0.71	0.07	n.d.		n.d.		n.d.	
Gd_2O_3	0.39	0.03	n.d.		0.20	0.02	n.d.		n.d.		n.d.	
Dy_2O_3	n.d.		n.d.		0.98	0.08	n.d.		n.d.		n.d.	
Er_2O_3	n.d.		n.d.		0.59	0.05	n.d.		n.d.		n.d.	
Yb_2O_3	n.d.		n.d.		0.74	0.06	n.d.		0.08	0.01	n.d.	
F	8.60	7.05	6.70	5.43	7.81	6.48	7.15	6.04	6.72	5.57	4.59	3.78
O=F	-3.62		-2.82		-3.29		-3.01		-2.83		-1.93	
O		29.84		29.92		29.67		30.23		30.61		31.80
Total	98.43		95.95		97.08		95.84		96.74		95.58	
Σ anions***		36.90		35.36		36.15		36.27		36.18		35.58
Σ cations****		16.45		15.55		15.88		15.67		15.90		23.67

* Calculated on the basis of 8 Si. ** Not detected. *** Ideal sum is 36. **** Ideal sum is 16.

Crystals used for single-crystal X-ray measurements were selected after optical inspection in order to avoid grains containing multiple crystallites. The ranges of the largest and smallest dimensions of the investigated crystals were respectively 0.11 to 0.18 mm and 0.02 to 0.07 mm. The crystals were mounted on a Bruker AXS four-circle diffractometer equipped with a CCD 1000K area detector and a flat graphite monochromator using Mo$K\alpha$ radiation from a fine-focus sealed X-ray tube. Reflections used for unit-cell determination were measured with long-duration exposures in search of weak superstructure reflections. This is an important aspect in identifying the different members of the group, since cation ordering may cause a doubling of the *b* axis, as is seen in rosenbuschite. Unit-cell determination and data collection were done in the SMART system of programs. Using ω- and ϕ-scans with a step size of 0.25°, intensities were measured for reflections within the θ range of 3.9° and 35°. The data collection of sample #531136 was done under different standard settings, and reflections were only measured for θ below 24°. Integrated intensities were calculated using the program SAINT. XPREP was used for unit-cell determination and calculation of intensities corrected for absorption. The $|E^2-1|$ value (Table 2) indicated all the triclinic structures to be centrosymmetric. However, Rastsvetaeva *et al.* (1995) found hainite (described as giannetite) to have crystallized in *P*1, and our datasets were therefore processed in each of the space groups, and the structures were further refined. In all cases, no significant differences between the acentric and the centrosymmetric models were observed, and all structures were concluded to be in $P\bar{1}$. The symmetry of seidozerite is *P*2/*n* in accordance with Simonov & Belov (1960). During the semiempirical absorption-corrections, crystal 1993.158 was modeled as a lamina parallel to (001), and the shape of the other crystals was fitted by an ellipsoid. Unit-cell dimensions and internal *R*-values after the corrections are given in Table 2.

Refinement procedure

Full-matrix least-squares refinements on F^2 were carried out in the SHELXL–97 program. Initial atom coordinates were taken from Cannillo *et al.* (1972) [götzenite], Shibaeva *et al.* (1964) [rosenbuschite] and Simonov & Belov (1960) [seidozerite], and refined isotropically. Site-occupancy factors (s.o.f.) were refined for all cation positions (the so-called *M* positions) except for the silicon positions. For atom positions on which the s.o.f. was found to differ significantly from unity after a first refinement, a weighted sum of X-ray scattering factors for two types of elements was used, and the sum of the two elements was constrained to be unity. All atoms were modeled anisotropically, and the s.o.f. for the Si, O, F positions were in turn set free, but all refined close to unity and were subsequently constrained to full occupancy. The distribution of O and F was estimated using bond-valence calculations and incorporated in a second refinement procedure. Finally, an isotropic secondary extinction was applied, but no improvement of the results was observed. Unit cells and statistical values for the refinements are given in Table 2. Refined atom coordinates for samples WBC–13, LF–A5 and 1993.158, which represent the three structure variants of the group, are given in Table 3. Observed and calculated structure-factors for all samples have been submitted to the Depository of Unpublished Data, CISTI, National Research Council of Canada, Ottawa, Ontario K1A 0S2, Canada.

TABLE 2. UNIT-CELL DIMENSIONS, INTERNAL R-VALUES AND REFINEMENT-DATA FOR ROSENBUSCHITE-GROUP SAMPLES

Mineral Space group	WBC-13 Götzenite $P\bar{1}$	WBC-12 Kochite $P\bar{1}$	LF-A2 Hainite $P\bar{1}$	LF-A5 Rosenbuschite $P\bar{1}$	TYROS Rosenbuschite $P\bar{1}$	1993.158 Seidozerite *P*2/*c*
a (Å)	9.6192(7)	10.032(2)	9.6079(7)	10.137(2)	10.108(1)	5.5558(3)
b (Å)	5.7249(4)	11.333(2)	5.7135(5)	11.398(2)	11.375(1)	7.0752(4)
c (Å)	7.3307(5)	7.202(1)	7.3198(5)	7.2714(12)	7.2620(9)	18.406(1)
α (°)	89.921(2)	90.192(4)	89.916(2)	90.216(3)	90.165(4)	
β (°)	101.132(2)	100.334(5)	101.077(2)	100.308(4)	100.311(3)	102.713(1)
γ (°)	100.639(2)	111.551(4)	100.828(2)	111.868(4)	111.911(3)	
N_{coll} *	5448	9277	4459	11647	4833	7866
R_{int}	0.040	0.036	0.039	0.056	0.045	0.044
Data	3005	5529	2283	5895	2174	2099
Parameters	145	287	144	287	287	144
$\lvert E^2-1 \rvert$	1.064	1.272	1.060	1.190	1.268	1.067
R(F)	4.0	4.0	3.7	4.9	3.2	2.7
$wR(F^2)$**	8.5	7.8	8.1	8.5	8.2	6.5
Goof***	1.014	1.027	1.016	1.045	1.002	1.066
$\Delta\rho_{max}$	0.84	0.93	0.88	1.34	0.61	0.56
$\Delta\rho_{min}$	-1.57	-1.11	-0.78	-0.94	-0.47	-1.05

* Number of reflections collected. ** *R*(F) for $F_o > 4\sigma F_o$, $wR(F^2)$ for all data. *** Goodness of fit.

Site-assignment procedure

The models of cation distributions presented here are based on chemical composition and refined site-scattering values. In the site-assignment procedure, all atom positions are assumed to be fully occupied, and the electron density of the assigned mixed occupancy has to equal the site-scattering values (expressed in electrons per formula units, *epfu*). In an iterative process, trial values were assigned to the occupancies (in atoms per formula unit, *apfu*), and the resulting models were evaluated using three distinct criteria:

1) A comparison of the composition of the model with the empirical formula. It should be noted that two distinct crystals were used for the chemical analysis and the analysis of the structure, respectively, and these may show minor differences.

2) A weighted bond-valence sum (BVS) was calculated for each site (parameters used are from Breese & O'Keeffe 1991) and compared with the corresponding valence-sum (VS).

3) Furthermore, a weighted ideal bond-length was calculated for each cation polyhedron using the ionic radii given by Shannon (1976) and compared with the average bond-length.

On the basis of present data, it is not possible to distinguish between the light and heavy rare-earth elements, and they are assigned using a weighted mean atomic number, but the bond-valence parameter and ionic radius of Ce were chosen as being representative of the observed REE mean. The results are given in Table 4.

Fluorine and oxygen are distributed over nine crystallographically distinct positions in götzenite, hainite and seidozerite, and 18 in rosenbuschite and kochite. The site assignment was guided by bond-valence calculations summarized in Table 5. The calculation indicated that all anion positions bonded to silicon (*O*1 to *O*7) are fully occupied by oxygen, and *F*9 is fully occupied by fluorine. *X*8 is a mixed oxygen–fluorine site, and the ratio between the anions on these sites is determined by the best fit between BVS and VS.

CRYSTALLOGRAPHY

General description of the crystal structure of götzenite and hainite

The crystal structure of götzenite is triclinic (Fig. 1). In principle, the structure is a framework of edge- and

TABLE 3. ATOM COORDINATES AND ISOTROPIC TEMPERATURE-FACTORS FOR SAMPLES WBC-13, LF-A5 AND 1993.158

site	*N*	*x*	*y*	*z*	U_{iso}
WBC-13 götzenite					
*M*1	2	0.63094(5)	0.22638(8)	0.90950(5)	0.0110(1)
*M*2	2	0.99344(9)	0.4966(1)	0.24160(9)	0.0186(2)
*M*3	2	0.63285(6)	0.2274(1)	0.40744(6)	0.0168(2)
*M*4	1	0	0	0.5	0.0153(4)
*M*5	1	0	0	0	0.0243(3)
*Si*1	2	0.71688(8)	0.7504(1)	0.6519(1)	0.0091(1)
*Si*2	2	0.72432(8)	0.7551(1)	0.2148(1)	0.0094(1)
*O*1	2	0.7583(2)	0.7860(4)	0.4440(3)	0.0233(5)
*O*2	2	0.6152(2)	0.9402(3)	0.6688(3)	0.0145(4)
*O*3	2	0.6188(2)	0.9363(3)	0.1415(3)	0.0171(4)
*O*4	2	0.6436(3)	0.4773(4)	0.6670(3)	0.0238(5)
*O*5	2	0.6660(3)	0.4790(4)	0.1607(3)	0.0288(5)
*O*6	2	0.8757(2)	0.8129(3)	0.7855(3)	0.0170(4)
*O*7	2	0.8856(2)	0.8355(3)	0.1717(3)	0.0165(4)
*X*8	2	0.8852(2)	0.2592(3)	0.9675(2)	0.0216(4)
*F*9	2	0.8856(2)	0.3062(3)	0.4759(2)	0.0187(4)
LF-A5 rosenbuschite					
*M*1a	2	0.35393(6)	0.28239(5)	0.08742(7)	0.0106(1)
*M*1b	2	0.3643(1)	0.78976(9)	0.0898(1)	0.0131(3)
*M*2a	2	0.0056(2)	0.2549(1)	0.7546(2)	0.0249(6)
*M*2b	2	0.9957(1)	0.2524(1)	0.2457(2)	0.0235(5)
*M*3a	2	0.3576(1)	0.2884(1)	0.5887(2)	0.0190(4)
*M*3b	2	0.3685(1)	0.7925(1)	0.5899(1)	0.0176(4)
*M*4a	1	0	0	0.5	0.0156(8)
*M*4b	1	0	0.5	0.5	0.025(1)
*M*5a	1	0	0	0	0.0120(3)
*M*5b	1	0	0.5	0	0.0199(4)
*Si*1a	2	0.2869(1)	0.0148(1)	0.3482(2)	0.0112(3)
*Si*2a	2	0.2823(1)	0.0128(1)	0.7895(2)	0.0111(3)
*Si*1b	2	0.2895(1)	0.5121(1)	0.3466(2)	0.0121(3)
*Si*2b	2	0.2887(1)	0.5092(1)	0.7925(2)	0.0123(3)
*O*1a	2	0.2668(4)	0.0320(4)	0.5648(5)	0.030(1)
*O*1b	2	0.2659(4)	0.4947(4)	0.5640(5)	0.035(1)
*O*2a	2	0.3785(4)	0.1595(3)	0.3066(5)	0.0175(8)
*O*2b	2	0.3905(4)	0.6583(3)	0.3360(5)	0.0186(8)
*O*3a	2	0.3785(4)	0.1557(3)	0.8846(5)	0.0217(8)
*O*3b	2	0.4024(4)	0.6533(3)	0.8609(5)	0.0193(8)
*O*4a	2	0.3650(4)	0.9166(3)	0.3357(5)	0.0249(9)
*O*4b	2	0.3585(4)	0.4096(3)	0.3020(5)	0.0249(9)
*O*5a	2	0.3452(4)	0.9064(3)	0.8387(5)	0.0243(9)
*O*5b	2	0.3444(4)	0.3984(3)	0.8680(5)	0.0243(9)
*O*6a	2	0.1236(4)	0.9616(3)	0.2279(5)	0.0225(8)
*O*6b	2	0.1250(4)	0.4707(3)	0.2272(5)	0.0224(8)
*O*7a	2	0.1166(3)	0.9666(3)	0.8194(5)	0.0195(8)
*O*7b	2	0.1285(4)	0.4799(3)	0.8320(5)	0.0243(8)
*X*8a	2	0.1308(3)	0.1890(3)	0.0365(4)	0.0146(7)
*X*8b	2	0.1129(3)	0.6864(3)	0.0331(4)	0.0303(8)
*F*9a	2	0.1119(3)	0.2089(3)	0.5239(4)	0.0287(8)
*F*9a	2	0.1218(3)	0.7054(3)	0.5275(5)	0.0319(8)
1993.158 seidozerite					
*M*1	4	0.19770(4)	0.11864(3)	0.07405(1)	0.0085(1)
*M*2a	2	0.5	0.35047(9)	0.25	0.0121(2)
*M*2b	2	0.5	0.8502(1)	0.25	0.0188(4)
*M*3	4	0.2020(2)	0.6124(1)	0.06966(5)	0.0162(3)
*M*4	2	0	0.6105(2)	0.25	0.0157(4)
*M*5	2	0	0.11058(7)	0.25	0.0093(2)
*Si*1	4	0.7228(1)	0.38351(8)	0.10434(3)	0.0087(1)
*Si*2	4	0.7187(1)	0.84173(8)	0.10434(3)	0.0083(1)
*O*1	4	0.7337(3)	0.6129(2)	0.10876(9)	0.0172(4)
*O*2	4	0.9265(3)	0.3211(2)	0.05873(8)	0.0119(3)
*O*3	4	0.9022(3)	0.9102(2)	0.05111(8)	0.0113(3)
*O*4	4	0.4439(3)	0.3188(2)	0.06562(8)	0.0142(3)
*O*5	4	0.4353(3)	0.9037(2)	0.07700(9)	0.0139(3)
*O*6	4	0.7873(3)	0.3109(2)	0.19029(8)	0.0127(3)
*O*7	4	0.8201(3)	0.9136(2)	0.18927(8)	0.0130(3)
*X*8	4	0.2364(3)	0.1267(2)	0.18400(9)	0.0134(3)
*F*9	4	0.3052(3)	0.5767(2)	0.19223(8)	0.0224(3)

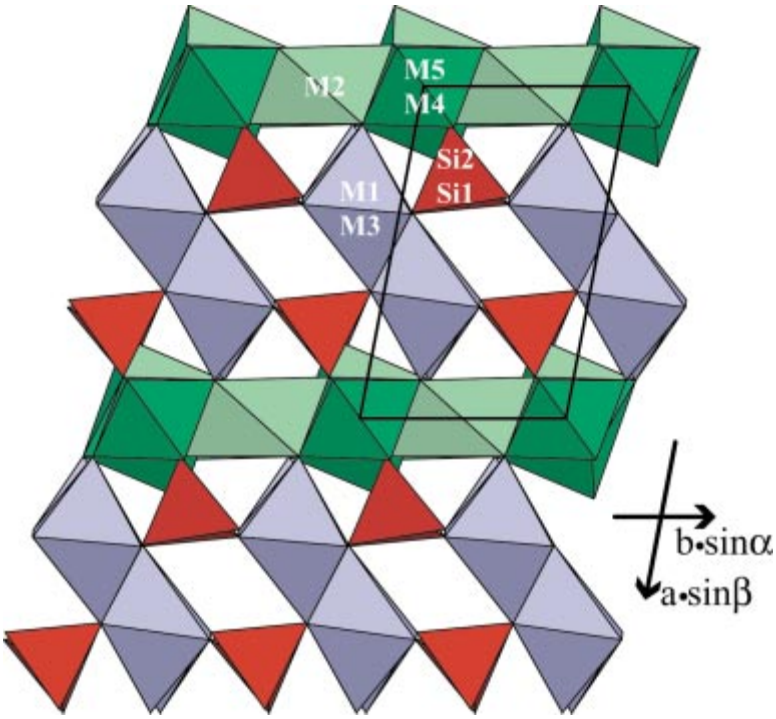

FIG. 1. The crystal structure of götzenite viewed along [001]. The cation positions are indicated.

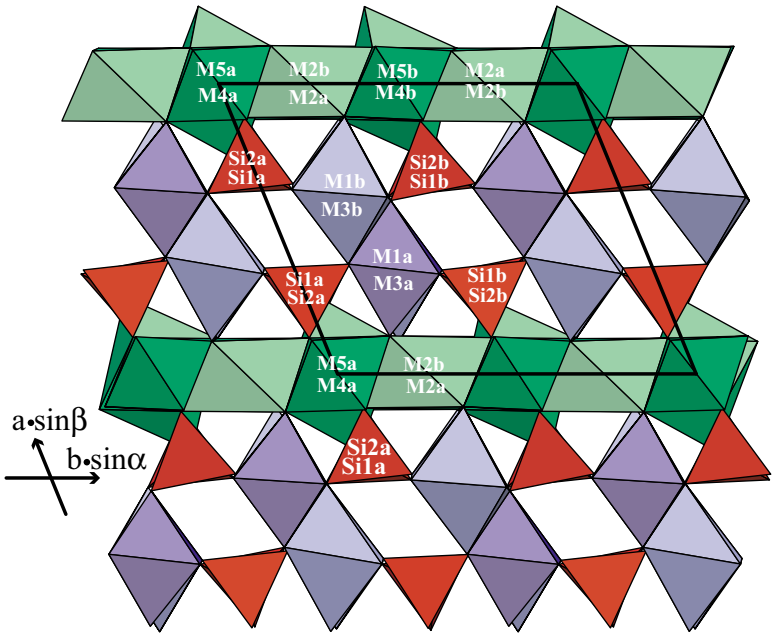

FIG. 2. The crystal structure of rosenbuschite (sample LF–A5) seen parallel to the *c* axis.

corner-sharing *M* octahedra hosting a variety of cations. The edge-sharing octahedra combine into (100) layers and into [001] ribbons, which are interconnected by sharing polyhedron vertices. Sorosilicate groups are situated in the hollows of the framework, with one set of vertices in common with a layer of octahedra, and the other two sets shared with ribbons of octahedra.

The [001] ribbon contains one type of octahedron column, in which two distinct octahedra (*M*1 and *M*3) alternate along the *c* axis. Centers of symmetry located on the edges of these octahedra generate an adjacent column, and the ribbon is thus two octahedra wide. The layer of octahedra (*O* layer) is composed of two distinct [001] columns. One contains only *M*2 octahedra mutually related by a center of inversion, and the other is composed of *M*5 octahedra and *M*4 polyhedra (CN = 8), both of which are positioned on centers of symmetry.

The double unit-cell of rosenbuschite and kochite

As Cannillo *et al.* (1972) pointed out, rosenbuschite and götzenite are in principle isostructural. However, in rosenbuschite (Fig. 2), cation order in the *M*1, and occasionally also in the *M*5 positions, results in a unit cell doubled in comparison to that of götzenite, the unit-cell transformation matrix from götzenite to rosenbuschite

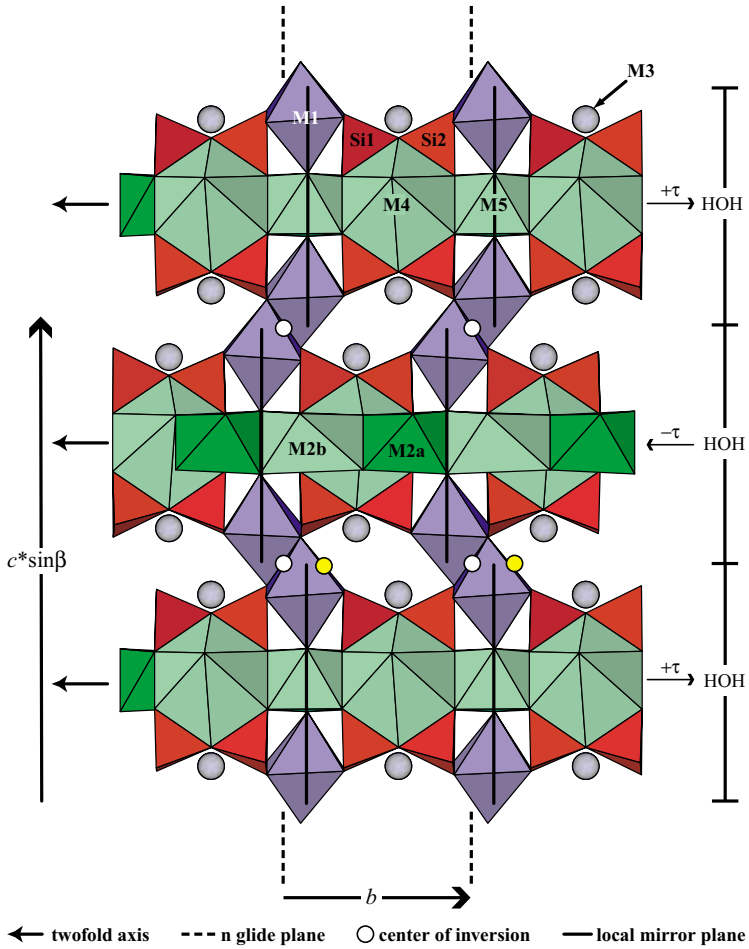

FIG. 3. The crystal structure of the monoclinic seidozerite viewed parallel to the *a* axis. The *HOH* layers and stacking vectors (τ) are indicated to the right. Positions of relevant elements of symmetry in the whole structure are also indicated along with one set of the local mirror planes of the *HOH* layers. Coordination polyhedra around the *M*3 positions are not indicated. An alternative position to the center of symmetry relating the central and lower *HOH* layer is indicated in yellow, and represents the triclinic mode of stacking.

being [–1 –1 0 / 0 2 0 / 0 0 –1]. The symmetry remains $P\bar{1}$, but the double spacing between the centers of symmetry also doubles the number of crystallographically independent positions when compared to götzenite. Thus one position in götzenite corresponds to two in rosenbuschite, which in this work are indicated with suffixes a and b. In order to enhance the readability of this paper, these suffixes are left out in general, and are only indicated where a distinction between the relevant sites is needed.

Owing to the cation order at the *M*1 positions, the ribbon of octahedra is not centrosymmetric, but is composed of two distinct columns of octahedra. The adjacent ribbons are related by centers of inversion, and the a and b columns are thus alternately positioned as the "upper" and "lower" column (Fig. 2). In the column composed of *M*2 octahedra, no center of symmetry is present, and this column is thus composed of two crystallographically distinct octahedra. The two other columns are composed of *M*4a + *M*5a and *M*4b + *M*5b polyhedra, in which all central cations have site symmetry $\bar{1}$.

The polytypic relationship to seidozerite

The crystal structure of seidozerite (Fig. 3) is monoclinic. Owing to different axial settings, the *a* axis of seidozerite corresponds to *b* of götzenite and $b_{\text{seidozerite}}$ corresponds to $c_{\text{götzenite}}$. The unit cell of götzenite may be transformed into that of seidozerite (approximately) by [0 1 0 / 0 0 –1 / –2 –½ –1].

Christiansen *et al.* (1999) pointed out the polytypic relationship between götzenite–rosenbuschite and seidozerite. They are considered two maximally ordered polytypes in the configurational or heterochemical sense (Makovicky 1997) in that the chemical compositions of the minerals differ significantly. If one forgets about the chemical compositions, the two structures can be considered as stackings of identical *HOH* layers parallel to (001) (in the axial setting of seidozerite), as shown on Figure 3. The layers are bordered by planes cutting through the ribbons of octahedra, and each *HOH* layer is thus composed of an *O* layer sandwiched between two heterogeneous layers (*H* layers) comprising the Si_2O_7 groups and *M*(1,3) octahedra. The pseudosymmetry of

TABLE 4. SITE-SCATTERING VALUES (*epfu*), SITE ASSIGNMENT (*apfu*), COORDINATION NUMBER (CN), BOND-VALENCE* SUM (BVS), VALENCE SUM (VS), AVERAGE BOND-LENGTHS (ABL) AND IDEAL** BOND-LENGTHS (IBL) FOR ROSENBUSCHITE-GROUP MINERALS

site	*epfu*	*apfu*	CN	BVS	VS	ABL	IBL
WBC-13 (götzenite)							
*M*1	48.2	$Ca_{1.62}REE_{0.13}Mn_{0.11}Zr_{0.09}Y_{0.06}$	6	2.16	2.18	2.344	2.344
*M*2	32.9	$Ca_{1.22}Na_{0.78}$	6	1.44	1.61	2.370	2.347
*M*3	44.5	$Ca_{1.88}REE_{0.12}$	6	1.82	2.06	2.412	2.366
			7	1.88	2.06	2.494	2.428
*M*4	12.7	$Na_{0.81}Ca_{0.19}$	8	1.44	1.19	2.470	2.471
*M*5	22.8	$Ti_{0.92}Fe_{0.05}Nb_{0.03}$	6	3.80	3.94	1.972	1.977
WBC-12 (kochite)							
*M*1a	68.5	$Zr_{1.35}Ca_{0.41}Fe_{0.24}$	6	3.29	3.36	2.148	2.162
*M*1b	49.2	$Mn_{1.09}Ca_{0.78}Ce_{0.07}Y_{0.05}$	6	2.01	2.06	2.294	2.276
*M*2a	26.5	$Na_{1.5}Ca_{0.5}$	6	1.29	1.25	2.366	2.362
*M*2b	29.8	$Na_{1.13}Ca_{0.87}$	6	1.46	1.43	2.353	2.359
*M*3a	35.3	$Ca_{1.48}Na_{0.52}$	6	1.47	1.74	2.444	2.370
			8	1.65	1.74	2.537	2.504
*M*3b	39.2	$Ca_{1.92}Na_{0.08}$	6	1.81	1.96	2.395	2.366
*M*4a	12.2	$Na_{0.86}Ca_{0.14}$	8	1.36	1.14	2.469	2.534
*M*4b	11.7	$Na_{0.92}Ca_{0.08}$	8	1.23	1.08	2.502	2.538
*M*5a	25.6	$Ti_{0.81}Nb_{0.13}Zr_{0.06}$	6	4.05	4.13	1.978	1.990
*M*5b	23.6	$Ti_{0.92}Nb_{0.08}$	6	3.96	4.08	1.970	1.976
LF-A2 (hainite)							
*M*1	59.2	$Ca_{1.2}Y_{0.31}REE_{0.21}Zr_{0.2}Mn_{0.08}$	6	2.46	2.46	2.312	2.316
*M*2	30.9	$Na_{1.01}Ca_{0.99}$	6	1.37	1.49	2.374	2.350
*M*3	42.4	$Ca_{1.94}REE_{0.06}$	6	1.75	2.03	2.417	2.362
			7	1.82	2.03	2.498	2.425
*M*4	12.5	$Na_{0.83}Ca_{0.17}$	8	1.36	1.17	2.482	2.472
*M*5	25.0	$Ti_{0.78}Nb_{0.08}Fe_{0.08}Zr_{0.06}$	6	3.78	3.92	1.986	1.993
LF-A5 (rosenbuschite)							
*M*1a	75.8	$Zr_{1.68}Ca_{0.28}Hf_{0.04}$	6	3.47	3.72	2.144	2.128
*M*1b	45.4	$Ca_{1.6}Mn_{0.22}Y_{0.15}Ce_{0.03}$	6	2.00	2.09	2.359	2.341
*M*2a	29.6	$Na_{1.15}Ca_{0.85}$	6	1.36	1.42	2.375	2.358
*M*2b	31.5	$Ca_{1.06}Na_{0.94}$	6	1.47	1.53	2.365	2.356
*M*3a	35.4	$Ca_{1.49}Na_{0.51}$	6	1.38	1.75	2.470	2.367
			8	1.59	1.75	2.545	2.501
*M*3b	39.0	$Ca_{1.89}Na_{0.11}$	6	1.78	1.95	2.399	2.363
*M*4a	12.7	$Na_{0.81}Ca_{0.19}$	8	1.37	1.19	2.477	2.531
*M*4b	12.3	$Na_{0.86}Ca_{0.14}$	8	1.24	1.14	2.518	2.534
*M*5a	35.6	$Zr_{0.67}Ti_{0.25}Nb_{0.08}$	6	4.07	4.08	2.045	2.058
*M*5b	25.8	$Ti_{0.7}Fe_{0.11}Zr_{0.1}Nb_{0.09}$	6	3.66	3.86	2.001	2.005
TYROS (rosenbuschite)							
*M*1a	74.3	$Zr_{1.6}Ca_{0.33}Y_{0.03}Hf_{0.03}$	6	3.41	3.65	2.151	2.138
*M*1b	45.2	$Ca_{1.58}Mn_{0.24}Y_{0.15}Ce_{0.03}$	6	2.03	2.09	2.352	2.339
*M*2a	28.9	$Na_{1.23}Ca_{0.77}$	6	1.33	1.38	2.375	2.357
*M*2b	30.9	$Na_{1.01}Ca_{0.99}$	6	1.45	1.50	2.363	2.355
*M*3a	36.1	$Ca_{1.57}Na_{0.43}$	6	1.43	1.78	2.462	2.366
			8	1.64	1.78	2.541	2.499
*M*3b	39.5	$Ca_{1.95}Na_{0.05}$	6	1.83	1.97	2.393	2.362
*M*4a	13.3	$Na_{0.74}Ca_{0.26}$	8	1.45	1.26	2.468	2.527
*M*4b	12.5	$Na_{0.83}Ca_{0.17}$	8	1.27	1.17	2.510	2.533
*M*5a	32.4	$Zr_{0.43}Ti_{0.43}Nb_{0.14}$	6	4.09	4.15	2.019	2.030
*M*5b	24.2	$Ti_{0.83}Nb_{0.11}Fe_{0.06}$	6	3.72	3.99	1.988	1.985
1993.158 (seidozerite)							
*M*1	139.6	$Zr_{2.77}Ti_{0.76}Fe_{0.36}Mg_{0.06}Nb_{0.05}$	6	3.75	3.80	2.080	2.072
*M*2a	40.7	$Mn_{0.85}Mg_{0.53}Fe_{0.28}Ca_{0.23}Na_{0.11}$	6	1.88	1.94	2.182	2.174
*M*2b	23.2	$Na_{1.87}Ca_{0.13}$	6	1.04	1.06	2.426	2.368
*M*3	45.5	$Na_{3.84}Ca_{0.16}$	6	1.05	1.04	2.449	2.381
			8	1.16	1.04	2.553	2.527
*M*4	21.8	$Na_{1.98}$	8	1.19	0.99	2.493	2.511
*M*5	44.8	$Ti_{1.96}Nb_{0.04}$	6	3.93	4.02	1.971	1.979

* Bond-valence parameters taken from Brese & O'Keeffe (1991). ** Ideal bond-lengths are calculated on the basis of the ionic radii of Shannon (1976). The bond lengths are quoted in Å; *epfu*: electrons per formula unit, *apfu*: atoms per formula unit.

the *HOH* layer is represented by the layer group *P* 1 2/*m* (1) with the two-fold axis parallel to *b*. On the boundary between the *M*1 octahedra, the two adjacent layers are related by a center of inversion displacing them by ¼*a* + ¼*b* (= τ). The symmetry of the single *HOH* layer generates an alternative position for the interlayer center of inversion, located on the opposite side of the local mirror (Fig. 3). In this way, the center of inversion may, after each *HOH* layer, be located in one of these two positions, changing only the direction of shift τ of the following, adjacent *HOH* layer. The local mirror plane stands perpendicular to the *b* axis, and it is only the *b* component of τ that is affected. In götzenite, the directions of τ are uniform, and the stacking of layers can in this way be represented as $+\tau_b+\tau_b$. In this stacking sequence, the local centers of inversion of the *HOH* layer are consistent for the whole structure, and götzenite thus has triclinic symmetry. Seidozerite is characterized by a stacking sequence of $+\tau_b-\tau_b$, in which the local two-fold axes become total ones, resulting in monoclinic symmetry. In this structure, the local centers of inversion within the *HOH* layers become extinct as a result, resulting in two crystallographically distinct *M*2 positions, situated on a two-fold axis (*M*2a and *M*2b). The *M*4 and *M*5 positions are also situated on a two-fold axis.

The present relationship has been described using the formalism for OD structures by Betti (1998) (S. Merlino, pers. commun.).

Overview of the Distribution of Cations

A graphical overview of the distribution of cations in the five specimens investigated is given in Figure 4. Each specimen represents a member in the rosenbuschite group (Table 4). Common to all members is the presence of sodium as the main occupant of the *M*4 site.

In götzenite (WBC–13), *M*1, *M*2 and *M*3 are all dominated by Ca, and Ti occupies *M*5. Substantial amount of Na enters the *M*2 position. In specimen LF–A2, the Na:Ca ratio just exceeds 1 in this particular site, whereas the remaining sites are dominated by the same cations. However, in the *M*1 position, only 60% of the occupants are Ca, because Y, REE and Zr also enter this site. The overall Na/Ca value of this specimen corresponds to that of hainite (Johan & Čech 1989), and we therefore consider LF–A2 as hainite. In the work of Rastsvetaeva *et al.* (1995), ordering of the two cations at two crystallographically distinct *M*2 positions causes a loss of centrosymmetry (see also Atencio *et al.* 1999). In the present work, no evidence of such order was observed. Samples WBC–13 and LF–A2 contain significant amounts of REE. This group of elements enters the *M*1 and *M*3 sites only. As pointed out by Christiansen & Rønsbo (2000), the concentration of REE in these positions plays a key role in the relationship of götzenite to the closely associated and REE-rich rinkite group. This relationship is beyond the scope of this paper.

In rosenbuschite (LF–A5 and TYROS), substantial amounts of Zr enter one of the two *M*1 positions, resulting in an ordering of Ca and Zr. *M*1a in this way is dominated by Zr, and *M*1b, by Ca. Order involving Ti and Zr also is observed in the two *M*5 positions, in that *M*5a contain significant amounts of Zr, and *M*5b is occupied by Ti. In sample LF–A5, *M*5a is clearly dominated by Zr, whereas the Zr/Ti value equals 1 in the type-locality rosenbuschite (TYROS). The type material is therefore ambiguous in defining whether rosenbuschite is Ti- or Zr-dominant in *M*5a. We recommend that rosenbuschite be considered Zr-dominant at this site, because the Zr–Ti order is observed in the type material of rosenbuschite, and a more advanced stage of this order is observed in specimen LF–A5.

In kochite (WBC–12), order at the *M*1 sites similar to that in rosenbuschite is observed. In this mineral, Zr also dominates the *M*1a site, whereas Mn and Ca enter the *M*1b site, with Mn as the dominant element. Kochite differs furthermore from sample LF–A5 and TYROS in that Ti is by far the dominant element at *M*5a.

The cation distributions in the remaining *M*2 and *M*3 sites are similar in all the variants of the rosenbuschite structure. Calcium is dominant at both the *M*3a and *M*3b sites. However, 25% of the *M*3a site is occupied by Na (Table 4), whereas *M*3b is fully occupied by Ca. In the *M*2 sites, the Na/Ca values are all close to one, except for the *M*2a in sample WBC–12, which contains 75% Na.

In seidozerite (1993.158), no cation order is observed at *M*1, and the site is dominated by Zr, with Ti and Fe as important substituents. Like kochite, seidozerite contains a Mn-dominant site. However, in seidozerite, Mn enters the *M*2a site, which also hosts minor amounts of Mg and Fe. Unlike the other members of the group, seidozerite is very poor in Ca. This is compensated for by a high content of Na, which is distributed over the *M*2b and *M*3 sites in addition to the *M*4 site. The *M*5 site is occupied by Ti. These results is in good agreement with the cation distribution found in a different specimen of seidozerite by Pushcharovskii *et al.* (2002) except for the *M*2b position, which in their specimen is dominated by Ca.

TABLE 5. BOND-VALENCE SUMS FOR SILICON AND ANION POSITIONS IN ROSENBUSCHITE-GROUP SAMPLES

	WBC-13	WBC-12		LF-A2	LF-A5		TYROS		1993.158
	götzenite	kochite		hainite	rosenbuschite		rosenbuschite		seidoz.
site*suffix*		*a*	*b*		*a*	*b*	*a*	*b*	*a*
Si1 *vu*	4.01	4.05	4.04	4.00	4.03	3.98	4.08	4.02	4.03
*Si*2	4.05	4.13	4.07	4.07	4.09	3.99	4.09	4.05	4.03
*O*1	2.19	2.24	2.18	2.20	2.21	2.15	2.22	2.14	2.20
*O*2	1.99	2.05	1.96	1.92	2.02	1.92	2.04	1.96	2.05
*O*3	1.96	1.95	1.89	2.00	1.96	1.86	1.98	1.89	1.92
*O*4	1.84	1.83	1.87	1.86	1.83	1.84	1.88	1.86	1.93
*O*5	1.93	1.86	1.98	1.96	1.94	1.96	1.95	1.99	2.02
*O*6	2.03	2.09	2.09	2.03	2.12	2.02	2.13	2.01	2.09
*O*7	2.03	2.16	2.07	2.03	2.19	2.02	2.20	2.03	2.14
*X*8*	1.25/	1.60/	1.38/	1.31/	1.66/	1.36/	1.62/	1.37/	1.70/
	1.25	1.7	1.5	1.3	1.7	1.4	1.6	1.4	1.7
*F*9	0.96	1.02	0.99	0.96	1.01	0.98	1.04	1.03	0.98

* Mixed site occupied by both oxygen and fluorine. The BVS/VS ratio is given. The results are expressed in valence units (*vu*). Seidoz.: seidozerite.

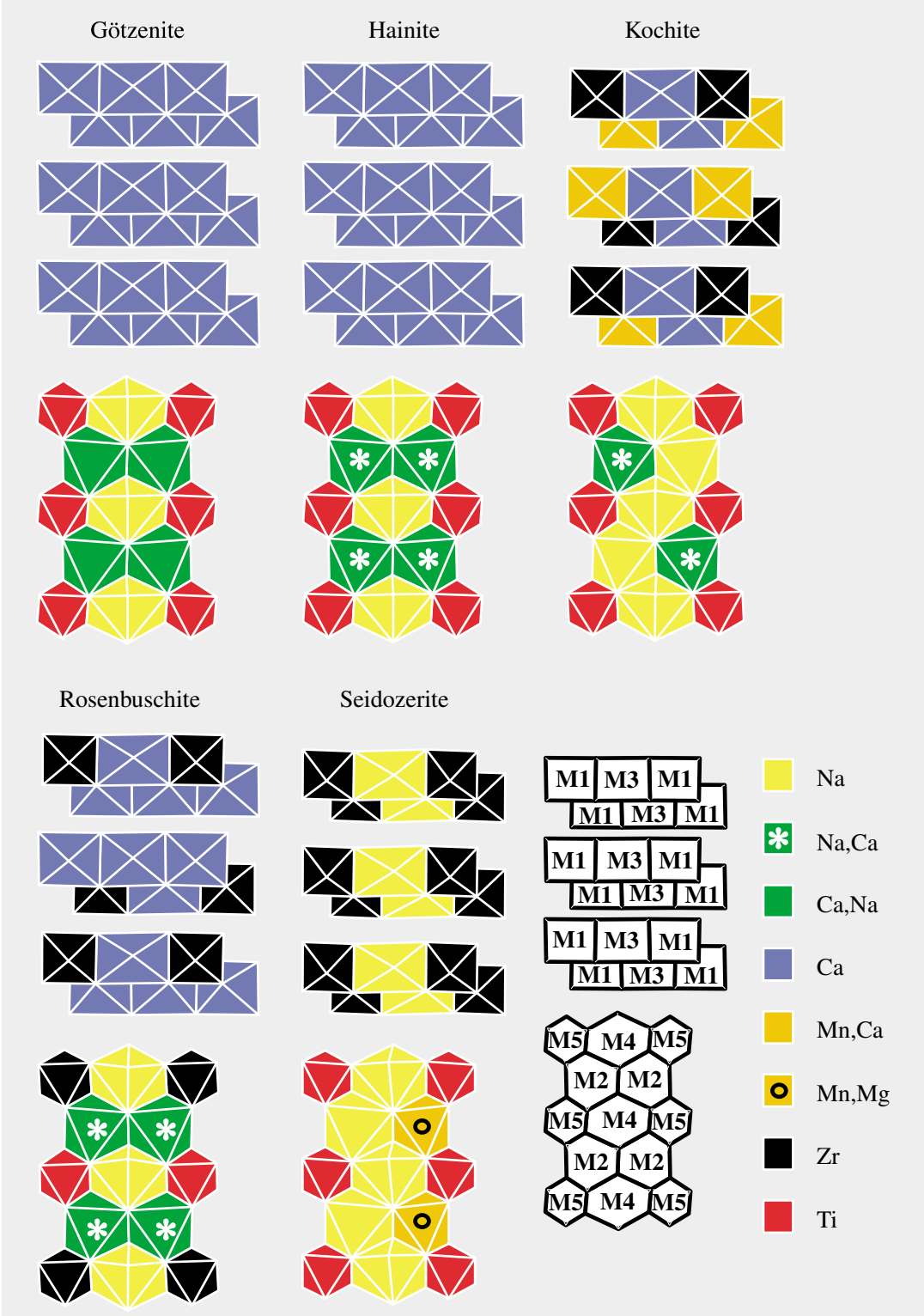
Götzenite
Hainite
Kochite
Rosenbuschite
Seidozerite
M1
M3
M1
M1
M3
M1
M5
M4
M5
M2
M2
Na
Na,Ca
Ca,Na
Ca
Mn,Ca
Mn,Mg
Zr
Ti

Discussion of the Sites

The variety of cations occupying the *M* positions in the rosenbuschite group of minerals have quite different ionic radii and valences. These cations are accommodated in coordination polyhedra of considerable differences in sizes and bond strengths. In order to combine these octahedra into edge-sharing ribbons and layers, a misfit between their ideal dimensions must be compensated for. In Table 6, a distortion parameter (υ) is given for each polyhedron. This parameter is defined as the deviation from the volume of an ideal polyhedron in percent (Makovicky & Balić-Žunić 1998). Not surprisingly, the relatively small and strongly bonded Si tetrahedra and Ti and Zr octahedra are close to being ideal (υ in the range 0.07–0.87%), whereas the larger Na and Ca polyhedra may be quite distorted (υ in the range 2.73–11.1%).

FIG. 4. The distribution of cations within the ribbons of octahedra (upper) and the layer of octahedra (lower) for the specimens of the rosenbuschite group investigated. The cation occupancies are represented by differently colored polyhedra. The setting of the figure corresponds to Figure 5. The scheme is inspired by Cannillo *et al.* (1972).

The M1 site

The *M*1 site is octahedrally coordinated to five atoms of oxygen and one mixed fluorine–oxygen site (*X*8). The five atoms of oxygen constitute the ligands

TABLE 6. BOND LENGTHS (Å), POLYHEDRON VOLUMES (Å^3) AND DISTORTION PARAMETERS* (%) FOR *M* POSITIONS IN SAMPLES WBC-13 (GÖTZENITE), LF-A5 (ROSENBUSCHITE) AND 1993.153 (SEIDOZERITE)

WBC-13		*M*1a-*O*5b	2.088(4)	*M*3b-*O*3b	2.590(4)	*M*2a-*F*9	2.088(2)
*M*1-*O*5	2.277(2)	*M*1a-*O*4b	2.109(4)	Vol[6]	17.52	*M*2a-*F*9	2.088(2)
*M*1-*O*4	2.291(2)	*M*1a-*O*2a	2.168(4)	υ[6]	4.26	*M*2a-*O*6	2.146(2)
*M*1-*O*3	2.368(2)	*M*1a-*O*3a	2.170(3)	*M*4a-*F*9a	2.213(3)	*M*2a-*O*6	2.146(2)
*M*1-*F*8	2.373(2)	*M*1a-*O*3b	2.257(4)	*M*4a-*F*9a	2.213(3)	*M*2a-*X*8	2.312(2)
*M*1-*O*2	2.374(2)	Vol[6]	12.97	*M*4a-*O*7a	2.509(4)	*M*2a-*X*8	2.312(2)
*M*1-*O*3	2.379(2)	υ[6]	0.79	*M*4a-*O*7a	2.509(4)	Vol[6]	13.34
Vol[6]	16.49	*M*1b-*O*5a	2.285(4)	*M*4a-*O*1a	2.545(4)	υ[6]	3.89
υ[6]	3.28	*M*1b-*O*4a	2.292(4)	*M*4a-*O*1a	2.545(4)	*M*2b-*O*7	2.343(2)
*M*2-*F*9	2.341(2)	*M*1b-*X*8b	2.331(3)	*M*4a-*O*6a	2.639(4)	*M*2b-*O*7	2.343(2)
*M*2-*F*9	2.347(2)	*M*1b-*O*2b	2.381(4)	*M*4a-*O*6a	2.639(4)	*M*2b-*F*9	2.353(2)
*M*2-*O*7	2.374(2)	*M*1b-*O*3a	2.416(4)	Vol[8]	24.57	*M*2b-*F*9	2.353(2)
*M*2-*F*8	2.376(2)	*M*1b-*O*3b	2.450(3)	υ[8]	7.69	*M*2b-*X*8	2.582(2)
*M*2-*O*6	2.384(2)	Vol[6]	16.91	*M*4b-*F*9b	2.191(3)	*M*2b-*X*8	2.582(2)
*M*2-*F*8	2.398(2)	υ[6]	2.76	*M*4b-*F*9b	2.191(3)	Vol[6]	17.45
Vol[6]	16.36	*M*2a-*F*9a	2.304(4)	*M*4b-*O*7b	2.584(4)	υ[6]	7.86
υ[6]	7.67	*M*2a-*O*6a	2.340(4)	*M*4b-*O*7b	2.584(4)	*M*3-*F*9	2.217(2)
*M*3-*O*5	2.344(2)	*M*2a-*X*8b	2.352(4)	*M*4b-*O*6b	2.620(4)	*M*3-*O*2	2.361(2)
*M*3-*F*9	2.343(2)	*M*2a-*F*9b	2.362(4)	*M*4b-*O*6b	2.620(4)	*M*3-*O*5	2.423(2)
*M*3-*O*4	2.357(2)	*M*2a-*O*7b	2.409(4)	*M*4b-*O*1b	2.676(4)	*M*3-*O*4	2.484(2)
*M*3-*O*2	2.359(2)	*M*2a-*X*8a	2.483(4)	*M*4b-*O*1b	2.676(4)	*M*3-*O*2	2.548(2)
*M*3-*O*2	2.533(2)	Vol[6]	16.81	Vol[8]	25.96	*M*3-*O*3	2.661(2)
*M*3-*O*3	2.534(2)	υ[6]	5.85	υ[8]	7.14	*M*3-*O*1	2.848(2)
*M*3-*O*1	2.986(2)	*M*2b-*F*9a	2.306(4)	*M*5a-*O*7a	2.038(3)	*M*3-*O*1	2.882(2)
Vol[6]	17.62	*M*2b-*O*7a	2.330(4)	*M*5a-*O*7a	2.038(3)	Vol[6]	17.70
υ[6]	5.26	*M*2b-*F*9b	2.344(4)	*M*5a-*O*6a	2.044(3)	υ[6]	9.31
Vol[7]	21.43	*M*2b-*O*6b	2.359(4)	*M*5a-*O*6a	2.044(3)	Vol[8]	26.20
υ[7]	6.76	*M*2b-*X*8b	2.365(4)	*M*5a-*X*8a	2.053(3)	υ[8]	9.88
*M*4-*F*9	2.225(2)	*M*2b-*X*8a	2.488(3)	*M*5a-*X*8a	2.053(3)	*M*4-*F*9	2.204(2)
*M*4-*F*9	2.225(2)	Vol[6]	16.54	Vol[6]	11.38	*M*4-*F*9	2.204(2)
*M*4-*O*1	2.379(2)	υ[6]	5.98	υ[6]	0.19	*M*4-*O*7	2.521(2)
*M*4-*O*1	2.379(2)	*M*3a-*F*9a	2.268(3)	*M*5b-*X*8b	1.992(3)	*M*4-*O*7	2.521(2)
*M*4-*O*7	2.547(2)	*M*3a-*O*2b	2.352(4)	*M*5b-*X*8b	1.992(3)	*M*4-*O*6	2.555(2)
*M*4-*O*7	2.547(2)	*M*3a-*O*5b	2.433(4)	*M*5b-*O*6b	2.004(4)	*M*4-*O*6	2.555(2)
*M*4-*O*6	2.728(2)	*M*3a-*O*4b	2.505(4)	*M*5b-*O*6b	2.004(4)	*M*4-*O*1	2.693(2)
*M*4-*O*6	2.728(2)	*M*3a-*O*2a	2.603(4)	*M*5b-*O*7b	2.008(3)	*M*4-*O*1	2.693(2)
Vol[8]	24.79	*M*3a-*O*3a	2.658(4)	*M*5b-*O*7b	2.008(3)	Vol[8]	25.03
υ[8]	6.12	*M*3a-*O*1a	2.712(4)	Vol[6]	10.68	υ[8]	7.88
*M*5-*O*7	1.957(2)	*M*3a-*O*1b	2.827(5)	υ[6]	0.11	*M*5-*O*7	1.923(2)
*M*5-*O*7	1.957(2)	Vol[6]	18.47	**1993.153**		*M*5-*O*7	1.923(2)
*M*5-*O*6	1.964(2)	υ[6]	7.70	*M*1-*X*8	1.988(2)	*M*5-*X*8	1.979(2)
*M*5-*O*6	1.964(2)	Vol[8]	26.08	*M*1-*O*4	1.999(2)	*M*5-*X*8	1.979(2)
*M*5-*F*8	1.995(2)	υ[8]	9.37	*M*1-*O*5	2.007(2)	*M*5-*O*6	2.011(1)
*M*5-*F*8	1.995(2)	*M*3b-*F*9b	2.277(3)	*M*1-*O*2	2.053(2)	*M*5-*O*6	2.011(1)
Vol[6]	10.2	*M*3b-*O*5a	2.318(4)	*M*1-*O*3	2.178(1)	Vol[6]	10.18
υ[6]	0.25	*M*3b-*O*4a	2.335(4)	*M*1-*O*3	2.257(2)	υ[6]	0.37
LF-A5		*M*3b-*O*2a	2.389(4)	Vol[6]	11.80		
*M*1a-*X*8a	2.071(3)	*M*3b-*O*2b	2.486(4)	υ[6]	0.67		

* Distortion parameter (Makovicky & Balić-Žunić 1998): $\upsilon = (V_i - V_r)/V_i{*}100$, V_i = ideal volume of polyhedron, V_r = real volume of polyhedron. The ideal polyhedra are octahedron for CN = [6], pentagonal bipyramid for CN = [7] and square antiprism with maximum volume for CN = [8].

common to the octahedra sharing edges with *M*1, and link furthermore to five tetrahedra. One *M*1 and three *M*3 octahedra are joined to the edges of the same *M*1 octahedron, whereas the mixed *X*8 site is shared with three octahedra in the *O* layer (Fig. 5).

Ca, Zr, Mn and Y are the main elements occupying the *M*1 sites, and the volumes of these octahedra are the most variable in the structures (Table 6).

The smallest *M*1 octahedron is to be found in seidozerite. It hosts primarily Zr (70%) and Ti (20%) and has a volume of 11.8 Å^3. The degree of distortion of the octahedron is 0.67%, and thus close to ideal. However, the individual Zr–O bonds vary within the octahedron, the bonds to the two ligands (*O*3) common to two *M*1 octahedra being longer (Fig. 6). Seidozerite is one of the very rare minerals in which two Zr octahedra share an edge, and the longer bonds to *O*3 compensate for the direct repulsion between the two Zr cations and for the overbonding of *O*3.

In the variants of the rosenbuschite structure, the two distinct *M*1 octahedra have significantly different volumes. The Zr-dominant *M*1a octahedron has a volume of ~13 Å^3, whereas the volume of the Ca-dominant *M*1b octahedron is ~17 Å^3. The *M*1b octahedron in kochite (WBC–12) is smaller (15.7 Å^3, not listed), in accordance with Mn as the dominant element at this site. The Zr-dominated *M*1a octahedra are slightly larger than the *M*1 of seidozerite, owing to minor incorporation of Ca.

With respect of volume (16.49 Å^3) and distortion, the Ca-dominant *M*1 octahedron in götzenite is almost identical to the *M*1b octahedron in rosenbuschite. The *M*1 octahedron in sample LF–A2 differs from the one in WBC–13 only by being slightly smaller (15.95 Å^3, not listed), owing to the incorporation of significant amounts of Y.

The M5 site

The *M*5 octahedron is part of the layer of octahedra, and shares the edges of four *M*2 octahedra and two *M*4 polyhedra. The four corners shared with the *M*4 polyhedra also link to four Si tetrahedra (Fig. 5). The two

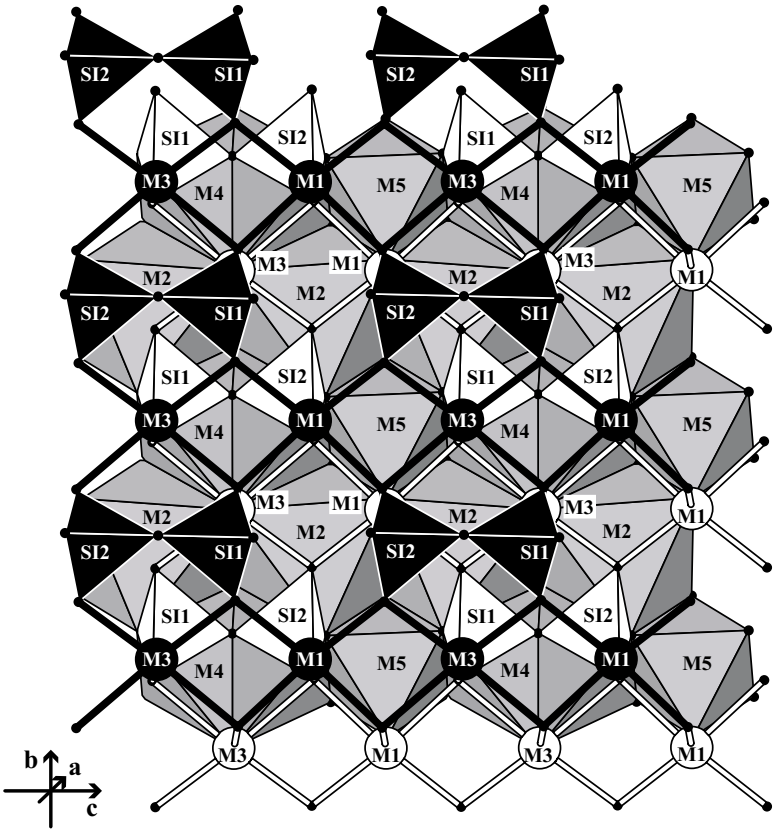

FIG. 5. The *O-H-H* layer of the götzenite structure projected onto (100). The *O* layers are indicated by grey polyhedra, whereas the tetrahedra, atoms and bonds shown in black and white indicate, respectively, the upper and lower *H* layers.

remaining ligands are the mixed *X*8 sites, which are also shared by *M*1 octahedra. Ti is by far the most common occupant of the site in rosenbuschite, though significant amounts of Zr are present. The volumes of the octahedra vary little, from 10.18 to 11.38 Å^3, the larger octahedra being occupied mainly by Zr.

The average bond-lengths of the Ti-dominated octahedra vary between 1.970 to 2.001 Å, which are longer than the ideal Ti$^{[6]}$–O$^{[4]}$ distance of 1.965 Å. Minor replacement of Ti by Fe, Nb and Zr partly explains this, but still a systematically deviation between the BVS and VS of these sites is observed (Table 4). This deviation is associated with high displacement-factors of Ti, which is elongate along the *X*8–*X*8 diagonal of the coordination octahedra, as shown in Figure 7a. If this phenomenon is interpreted as a static disorder, Ti would be displaced from the center of symmetry toward one of the corners, which changes the individual bond-lengths to an asymmetrical coordination. Figure 7b shows the estimated effect of such a displacement on the deviation of BVS and VS, and of the ideal and average bond-lengths. Note that the BVS is more sensitive to the displacement, whereas the average bond-length changes only slightly. The Zr-dominated *M*5 site has significantly lower displacement-factors and better VS–BVS balance.

The Si_2O_7 group

Table 7 lists some geometrical features of the Si_2O_7 groups. The average Si–O bond length for the tetrahe-

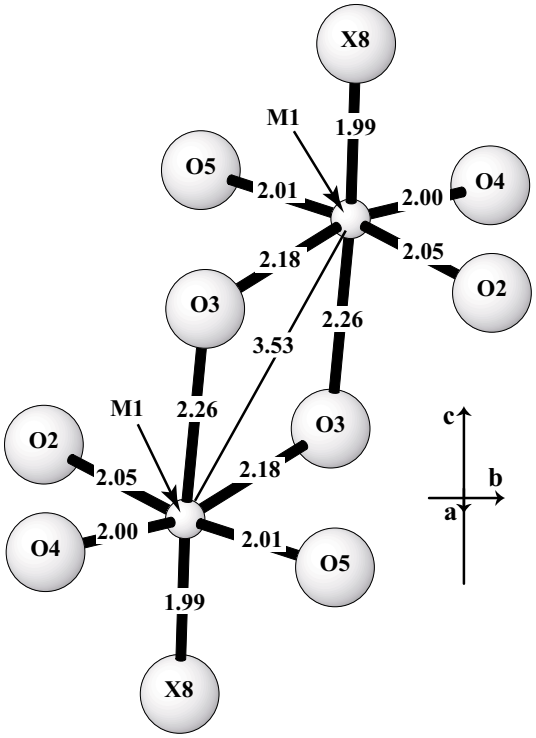

FIG. 6. The two edge-sharing Zr-bearing octahedra in seidozerite seen perpendicular to (001). Interatomic distances are given in Ångströms.

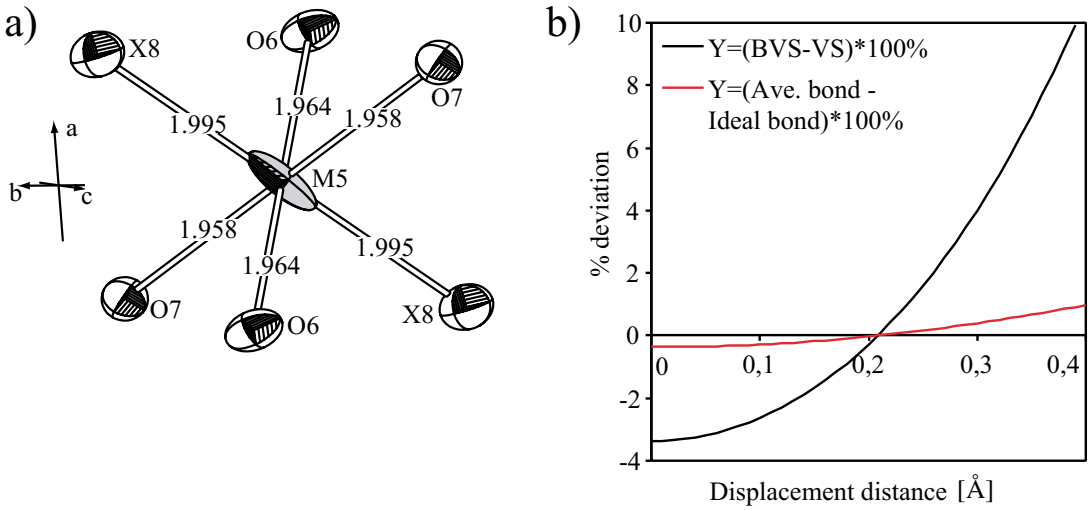

FIG. 7. a) Inclined view of the *M*5 polyhedron showing the central Ti cation and the coordinating anions as ellipsoids to indicate their thermal vibrations. Bond lengths are given in Å. Sample WBC–13 (götzenite) is shown. b) Graph showing the calculated effect of a displacement of the central Ti upon its bond-valence summation (BVS) and average bond-length. The basis for the calculation is an ideal octahedron with a bond length of 1.985 Å to the non-displaced Ti and a displacement direction toward X8. In this hypothetical case, Ti is likely to be displaced ~0.2 Å off the center.

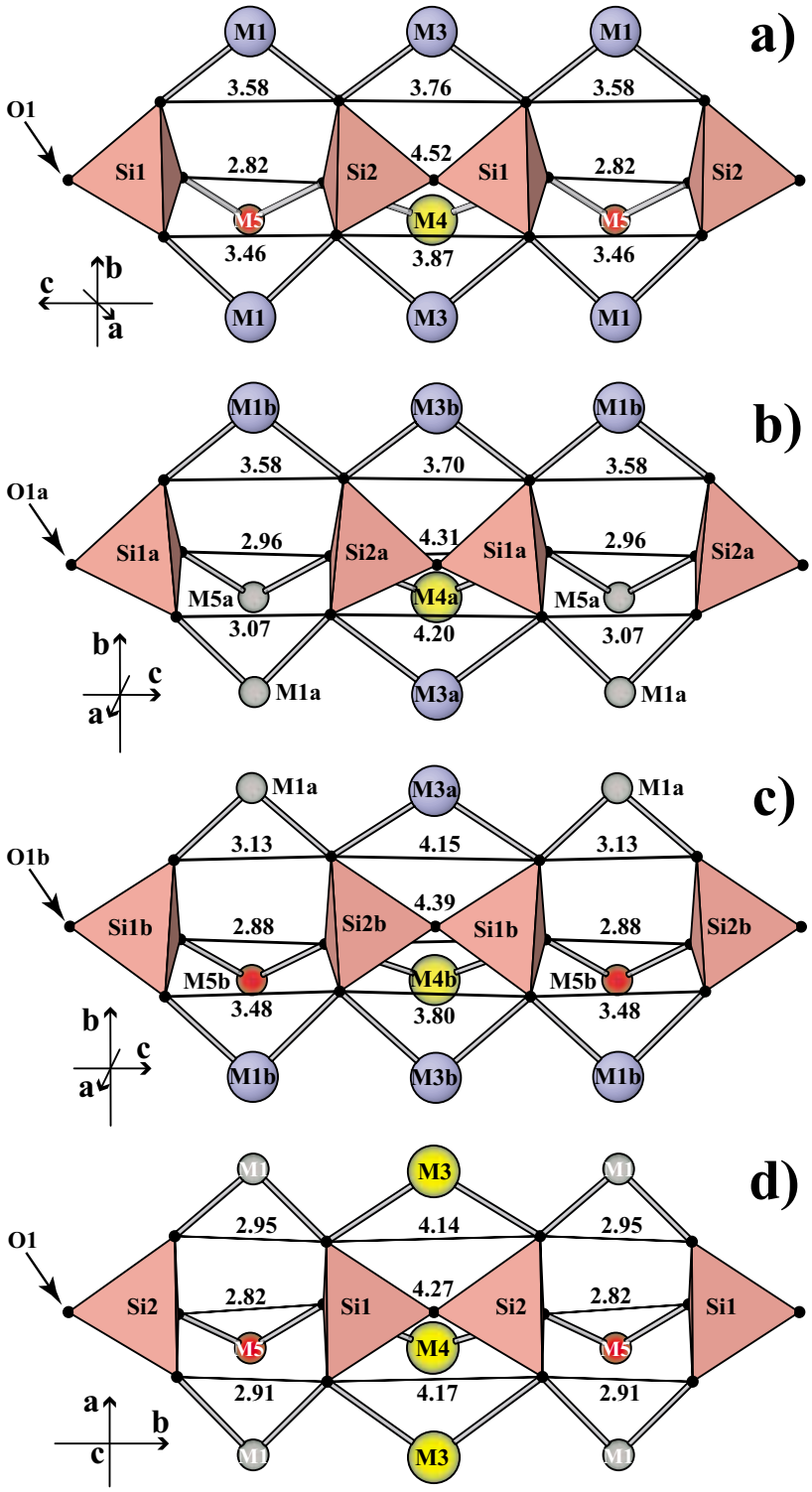

FIG. 8. The rows of disilicate groups along with their surrounding cations, showing the degree of distortion of the disilicate groups in relation to the size of the *M*1 and *M*5 cations. The letters represents a) WBC–13 [götzenite], b, c) LF–A5 [rosenbuschite], and d) 1993.158 [seidozerite]. The atoms are represented by blue (Ca), yellow (Na), grey (Zr) and red (Ti) spheres.

dra are within the ranges of 1.6162 to 1.6265 Å. The bonds to the bridging oxygen atoms (*O*1) are generally significantly longer than the remaining Si–O bonds, but in the seidozerite structure, no clear distinction among the bond lengths is apparent.

The BVS calculations invariably show evidence of overbonding of *O*1 by approximately 0.2 valence units (Table 5). A similar overbonding of the bridging oxygen has also been observed in members of the låvenite–wöhlerite group (Mellini 1981, Perchiazzi *et al.* 2000). As Mellini pointed out, these systematic deviations may be due to the correlation between bond valence and bond length, which does not take into account other parameters like bond angles and mutual screening among anions.

The Si–O–Si angle and the angles between the two basal planes of the Si_2O_7 dimers (Table 7) are closely related to the size of the *M*1 and *M*5 octahedra (Fig. 8). Two *M*1 and one *M*5 octahedra link the basal corners of adjacent disilicate groups, and any difference in size between the three octahedra sets the corners in one basal plane at different levels of *c*, resulting in an inclination between the two basal faces at the ends of the disilicate group. In seidozerite, the presence of three small Zr- and Ti-bearing octahedra result in a small inclination of 2.82°, whereas rosenbuschite and götzenite have, respectively, one and two large Ca octahedra in *M*1, re-

TABLE 7. BOND LENGTHS (Å), VOLUMES (Å^3) AND SELECTED OTHER PROPERTIES OF SiO_4 TETRAHEDRA AND Si_2O_7 GROUPS IN MINERALS OF THE ROSENBUSCHITE GROUP

Sample no.	WBC-13	WBC-12	WBC-12	LF-A2	LF-A5	LF-A5	1993.158
Si site	*Si*1	*Si*1a	*Si*1b	*Si*1	*Si*1a	*Si*1b	*Si*1
*O*1	1.651(2)	1.641(3)	1.643(3)	1.641(2)	1.644(4)	1.642(4)	1.626(1)
*O*2	1.611(2)	1.625(2)	1.605(3)	1.618(3)	1.624(3)	1.609(4)	1.612(2)
*O*4	1.605(2)	1.594(3)	1.618(2)	1.609(3)	1.604(4)	1.627(4)	1.622(1)
*O*6	1.626(2)	1.621(2)	1.618(2)	1.629(2)	1.614(3)	1.628(4)	1.626(1)
Ave.(4)	1.623	1.620	1.621	1.624	1.621	1.627	1.622
Volume	2.171	2.164	2.167	2.178	2.166	2.189	2.177
[001] rot.	5.56	3.13	5.71	4.78	2.61	6.21	2.76
Si site	*Si*2	*Si*2a	*Si*2b	*Si*2	*Si*2a	*Si*2b	*Si*2
*O*1	1.652(2)	1.627(3)	1.627(2)	1.644(2)	1.636(4)	1.635(4)	1.622(1)
*O*3	1.603(2)	1.614(2)	1.614(2)	1.611(3)	1.627(3)	1.628(3)	1.635(2)
*O*5	1.600(2)	1.590(3)	1.612(2)	1.600(3)	1.583(4)	1.625(4)	1.605(1)
*O*7	1.626(2)	1.620(3)	1.618(3)	1.618(3)	1.618(3)	1.611(3)	1.622(1)
Ave.(4)	1.620	1.613	1.618	1.618	1.616	1.625	1.621
Volume	2.156	2.133	2.156	2.153	2.142	2.185	2.174
[001] rot.*	9.20	7.31	10.78	8.51	6.43	11.27	9.69
Si-O-Si	154.1	161.3	163.7	157.9	157.6	163.6	173.3
Basal plane angle**	162.2	167. 7	167.9	164.6	165.9	167.4	177.2

* Rotation of tetrahedra around [001] (°), measured as the angle between (100) and the *O*2–*O*4 edge to *Si*1 and *O*3–*O*5 to *Si*2. ** Angle between basal faces (°) of the diorthosilicate groups. All volumes and angles are calculated using the program IVTON (Balić-Žunić &Vickovic 1986). Interconnected tetrahedra are listed in same column. Sample TYROS is not listed.

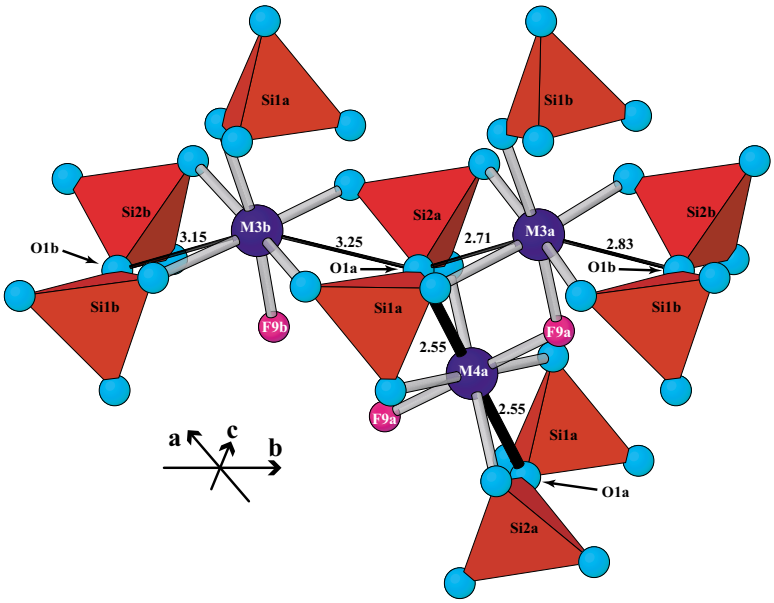

FIG. 9. A ball-and-stick model of the coordination polyhedra to the *M*3a, *M*3b and *M*4a positions in rosenbuschite (sample LF–A5), in an oblique view. The cation–*O*1 bonds are indicated in black, and their lengths are given in Å. Light blue and purple spheres represent O and F, respectively.

sulting in a larger inclination (12.6° to 17.77°). The difference between the Si–O–Si angle and the basal angle is due to distortion within the individual tetrahedra.

The M3 and M4 sites

Figure 8 also shows that the disilicate groups are riding on the edges of the *M*3 and *M*4 polyhedra. Each (*M*3, *M*4) polyhedron is attached to two disilicate groups. The distances between the pairs of vertices of the Si_2O_7 group and the *c* dimension of these polyhedra are thus coincident (Fig. 8). For the ideal Ca-bearing octahedron and Si_2O_7 group, this dimension would deviate by ~1 Å (3.34 and 4.32 Å, respectively). This misfit is compensated by bending the Si_2O_7 groups and by a high degree of distortion of the (*M*3, *M*4) polyhedra. The polyhedra are stretched along *c*, and in order to maintain realistic bond-lengths within the polyhedra, they are flattened perpendicular to the ribbon or layer. The edges shared with *M*1 or *M*5 become shorter in this way, and assume dimensions equal to that of a Zr or Ti octahedron. Owing to this stretch, ν is relative large for these octahedra, and varies between 4.26 and 11.1%.

The bridging oxygen (*O*1) in the disilicate group is located centrally between two *M*3 and one *M*4 positions. The distance to these three cations varies between 2.379 to 3.2 Å. This variation is geometrically correlated with the Si–O–Si angle, and its orientation. Since the obtuse part of the angle points in the direction of the *O layer*, the *O*1–*M*4 distance is the shorter of the three (2.379 to 2.693 Å). *M*4 is therefore considered to be in an eightfold coordination, which can best be described as a distorted hexagonal bipyramid. The distance to the two *M*3 positions is in the range 2.7 – 3.2 Å. In the structure of rosenbuschite variants (Fig. 9), the *O*1–*M*3a distance, ~2.8 Å, is significantly shorter than *O*1–*M*3b, ~3.2 Å. Correlated with this difference are also the distortion parameters for their octahedral coordination, ν being higher for the *M*3a octahedra and lower for the *M*3b octahedra. The occupancies of the two *M*3 positions also differ in that 25% Na enters *M*3a, whereas *M*3b is fully occupied by Ca. The *M*3a polyhedron shares edges with two high-charge Zr-bearing octahedra, whereas *M*3b is only linked to one, and a lower valence on the *M*3a site may therefore be preferred.

The M2 sites

The *M*2 positions are octahedrally coordinated by two *F*9, two *X*8 and two atoms of oxygen (*O*6 and *O*7), the oxygen atoms being shared with two SiO_4 tetrahedra. Through the two edges composed of the *F*9 and *X*8 ligands, *M*2 octahedra link into columns parallel to the *c* axis. Besides the edges shared with the two adjacent *M*2 octahedra, each *M*2 octahedron also shares edges with two relatively small *M*5 octahedra on one side and two larger *M*4 polyhedra on the other side (Fig. 5).

In the triclinic structures, the geometrical properties of the *M*2 octahedra are fairly constant, their volumes ranging between 16.27 and 16.81 $Å^3$, and the degree of distortion, between 5.9 and 7.7%. These octahedra plus the *M*2b octahedron in seidozerite all accommodate Na and Ca, whereas the *M*2a octahedron of seidozerite is occupied by Mn and Mg, and thus is significantly smaller (13.34 $Å^3$). As mentioned above, seidozerite deviates from the other members of the group by having only relatively small *M*1 octahedra, which results in a *b* dimension shorter than that in the triclinic structure-types (7.0752 Å *versus* 7.202–7.3307 Å). This difference is in accordance with the incorporation of a small Mn octahedron into the *M*2 column.

Discussion on the Solid Solution Involving the Members of the Rosenbuschite Group

Cannillo *et al.* (1972) introduced the idea of an isomorphous series between götzenite and seidozerite. Such a series would, however, imply fully replaceable Ca and Zr. Coupled with Ca–Zr substitution, the charge balance would be maintained by also substituting Ca by Na, and F by O. Two plots of chemical data (Fig. 10) show the degree of solid solution between these two end-members. A series of intermediate compositions exists between götzenite and rosenbuschite, whereas a compositional gap exists between rosenbuschite and seidozerite. In structures with mixed (Ca, Zr) occupancy of the *M*1 positions, half of the *M*1 positions thus are invariably occupied by Ca. Thus, two Zr octahedra need not share edges, as in seidozerite. The incorporation of a smaller Zr octahedron in *M*1 in the structure of rosenbuschite is compensated by adjusting the shape of surrounding polyhedra (especially the *M*3 positions) allowing, however, the same type of cations (Na, Ca) in these polyhedra. The two edge-sharing Zr-bearing octahedra in seidozerite lead to a pronounced contraction of the structure, which is furthermore enhanced by the presence of a Mn octahedron in one of the *M*2 sites. This configuration leads to the monoclinic mode of stacking of the *HOH* layers in seidozerite, whereas the triclinic mode of stacking characterizes the members with *M*1 fully or partially occupied by Ca. These geometrical differences result in a dimensional misfit between the rosenbuschite and seidozerite structures, which cannot be compensated, and the two configurational polytypes may not combine, resulting in the compositional gap observed in Figure 10.

The Role of Zirconium

A plot of Zr *versus* Ti + Nb is shown in Figure 11. Except for the composition of seidozerite, all points fall within one of two trends. For Zr < 1.5 *apfu*, the sum Ti + Nb has a fairly constant value, just below 2 *apfu*, whereas a negative 1:1 correlation is observed at higher

values of Zr. In the compositions poor in Zr, the *M*5 sites are occupied by Ti and Nb. With increasing Zr, the sum Ti + Nb remains unaffected because Zr enters the structure at the expense of Ca at the *M*1 site. At Zr > 1.5 *apfu*, the *M*1a site is saturated with respect of Zr, and this element now enters the structure at the expense of Ti. Notice that Ti does not drop below 1 *apfu* in the specimens examined, which indicates that one of the two *M*5 positions (*M*5b) is occupied by Ti. The sum of Ti, Zr and Nb never exceeds 4, which is in accordance with the total number of *M*1a and *M*5 sites in the unit cell of rosenbuschite.

The data plotted suggest two compositional series involving three end-members, one series between götzenite and kochite, which differ in Ca/Zr in the *M*1a sites, and another series between kochite and rosenbuschite, with variable Ti/Zr in the *M*5a site. Consequently, Figure 11 indicates that Zr enters the *M*5a site only in samples with a high Zr content at the *M*1a site. The relationship may, however, not be universal, as the chemical compositions of Ca-rich samples of götzenite indicate significant amounts of Zr in the *M*5 site (up to 25%) in the work of Sharygin *et al.* (1996).

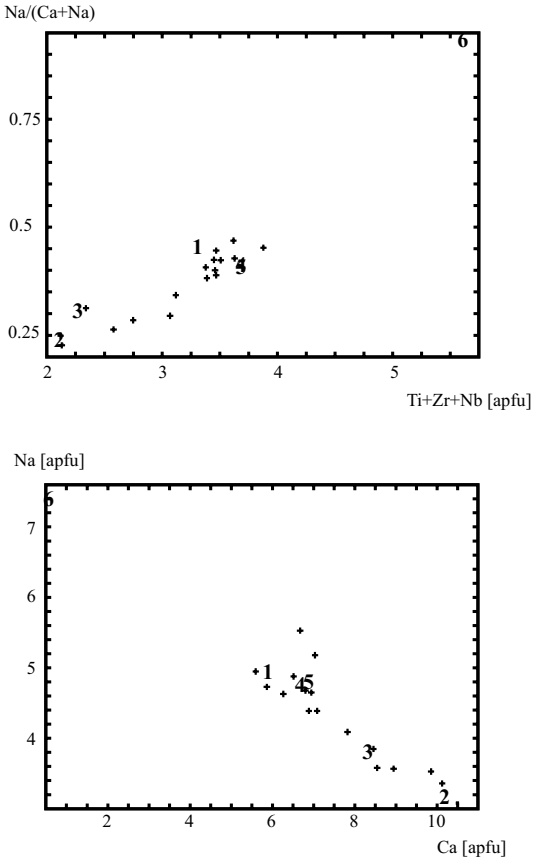

FIG. 10. a) Concentrations of Ti + Zr + Nb *versus* Na/(Ca + Na), and b) concentration of Ca *versus* that of Na, showing the compositional range of the specimens investigated. The numbers refer to the specimens investigated structurally: 1: WBC–12 (kochite), 2: WBC–13 (götzenite), 3: LF–A2 (hainite), 4: LF–A5 (rosenbuschite), 5: TYROS (rosenbuschite), and 6: 1993.158 (seidozerite).

The degree of order of Zr and Ti at the *M*5 sites in rosenbuschite can be correlated with the distribution of Zr and Ca at the *M*1 sites. In Figure 12, the two *M*5 octahedra are shown in relation with the *M*1 octahedra linked to their corners. The *M*5a octahedron is linked to two *M*1a octahedra through the *X*8a anion, and the *M*5b octahedron is linked to two *M*1b octahedra through *X*8b. As described above, the Zr-dominant *M*1a octahedron is considerably smaller than the Ca-dominant *M*1b octahedron. The contraction of the *M*1a octahedra has an expanding effect on the *M*5a octahedron, whereas the large *M*1b octahedra are combined with a slightly smaller *M*5b octahedron. As the ionic radius of Zr is slightly larger than Ti, the two cations are ordered at the two distinct *M*5 sites.

In addition to this finding, the oxygen:fluorine ratio in the *X*8a and *X*8b sites varies. *X*8a, which is bonded to Zr at the *M*1a site, is dominated by oxygen, and the *X*8b, bonded to Ca at the *M*1b site, is dominated by fluorine (Table 5). Thus the *M*5a position is primarily bonded to two atoms of oxygen in the *X*8 positions, whereas *M*5b primarily is bonded to fluorine, which differentiates the crystal-chemical character of the *M*5 positions even further.

THE TWO CONFIGURATIONAL POLYTYPES

The main crystal-chemical features of the rosenbuschite group of minerals have now been outlined. The existence of the two configurational polytypes remains to be explained. The two modes of stacking are each characterized by certain crystal-chemical properties. Especially important in this respect is the difference in size of *M*2a and *M*2b in seidozerite *versus* the fairly constant sizes of the *M*2 octahedra in the triclinic structures. A chain of arguments can be made by combining the sizes of the *M*2 octahedra with the rotations of the Si tetrahedra and the mode of stacking.

The monoclinic structure

The first step is to understand the relationship between sizes of the two *M*2 octahedra and the degree of rotation around [010] of the two tetrahedra attached to them. In seidozerite, the rotation of the *Si*1 tetrahedron is 2.76°, and the *Si*2 tetrahedron is rotated 9.69° (Table 7). As shown in Figure 13, the relatively small *M*2a octahedron is linked to two *Si*1 tetrahedra with a small degree of rotation, whereas the larger *M*2b octahedron is linked to two *Si*2 tetrahedra with a more pro-

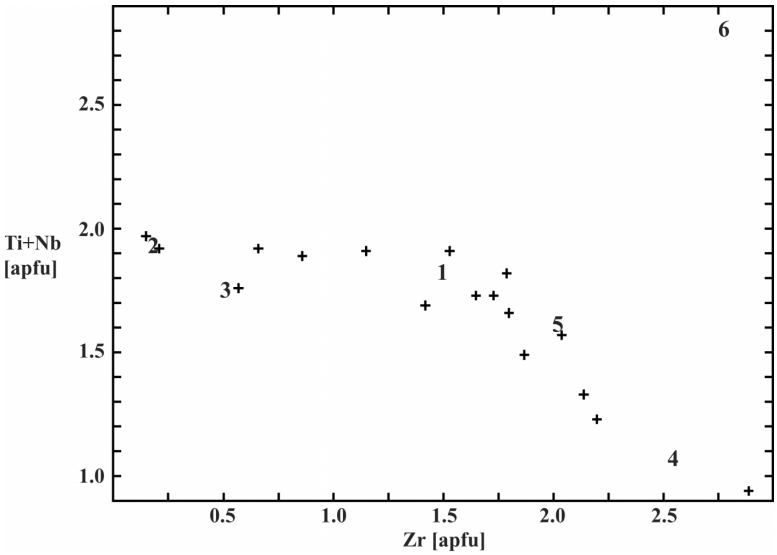

FIG. 11. Concentration of Zr *versus* that of Ti + Nb. Reference numbers as in Figure 10.

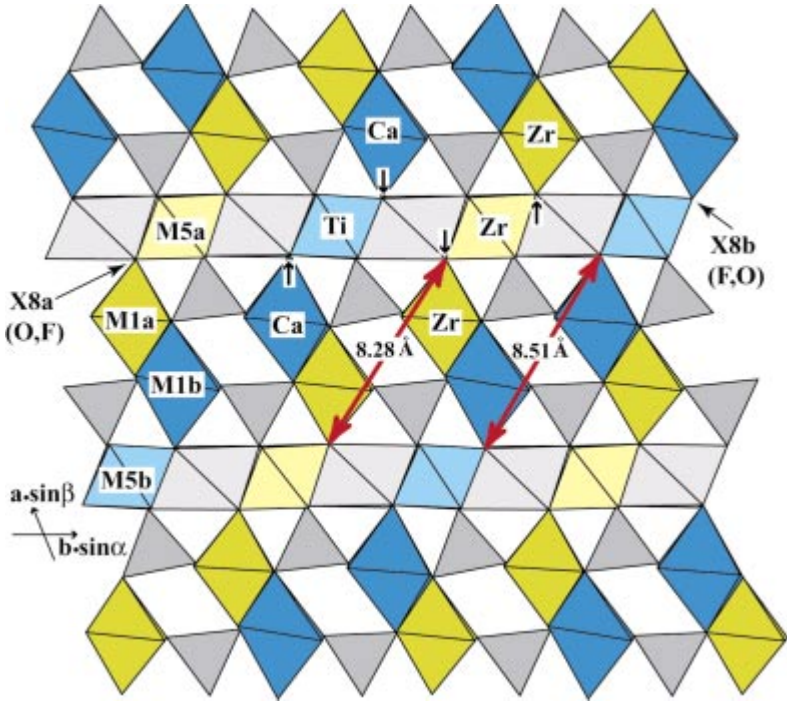

FIG. 12. Part of the structure of rosenbuschite seen along the *c* axis. The figure shows the relationship between the degree of order of the cations in the *M*1 and *M*5 octahedra. Black arrows indicate the direction of movement of the ligands from their "ideal" position. The dimensions are given in Å.

nounced rotation. The small rotation of the *Si*1 tetrahedron correlates in this way with a relatively shorter edge-length (*O*6–*X*8) of the *M*2a octahedron (3.30 Å), and the larger rotation of the *Si*2 tetrahedron correlates with a longer edge-length (*O*7–*X*8) of the *M*2b octahedron (3.56 Å). However, the configuration with the *Si*2 tetrahedra more rotated than the *Si*1 tetrahedra is valid for the whole group. The degree of rotation thus cannot only be due to the sizes of the *M*2 octahedra.

The two tetrahedra also differ in the attachment to the immediately adjacent *H*-layer. The *Si*1 tetrahedron is linked to the *M*3 octahedron (not shown in Fig. 13), and the *Si*2 tetrahedron is linked to the *M*1 octahedron. In Figure 13, the apex by which the *Si*2 tetrahedron is linked to the adjacent *H*-layer is indicated by a black circle (*O*3). A white arrow indicates that this point is pulled toward the relatively small *M*1 octahedra, causing a larger degree of rotation of the *Si*2 tetrahedron. The *Si*1 tetrahedron is attached to the relatively larger *M*3 octahedron (not shown in the figure), and thus has a smaller degree of rotation.

In seidozerite, the smaller size of the *M*2a octahedron is therefore best accommodated by being linked to two *Si*1 tetrahedra. The situation on both sides of an *HOH* layer thus will be equivalent, resulting in the displacement of two adjacent *HOH*-layers in the same direction (both $+\tau_b$ or $-\tau_b$) relative to the *HOH* layer sandwiched between them. This arrangement produces the monoclinic mode of stacking.

The triclinic structures

The triclinic structures are characterized by having uniform sizes of all *M*2 octahedra. The overall effects of the rotations of the tetrahedra are therefore not correlated with any difference in size of the *M*2 octahedra, as was observed in seidozerite. The respective enlargements and reductions resulting from the rotation of the tetrahedra are compensated by linking one *Si*1 tetrahedron with a relatively small rotation and one *Si*2 tetrahedron with a larger rotation to each *M*2 octahedron. Consequently, the displacements of the two adjacent

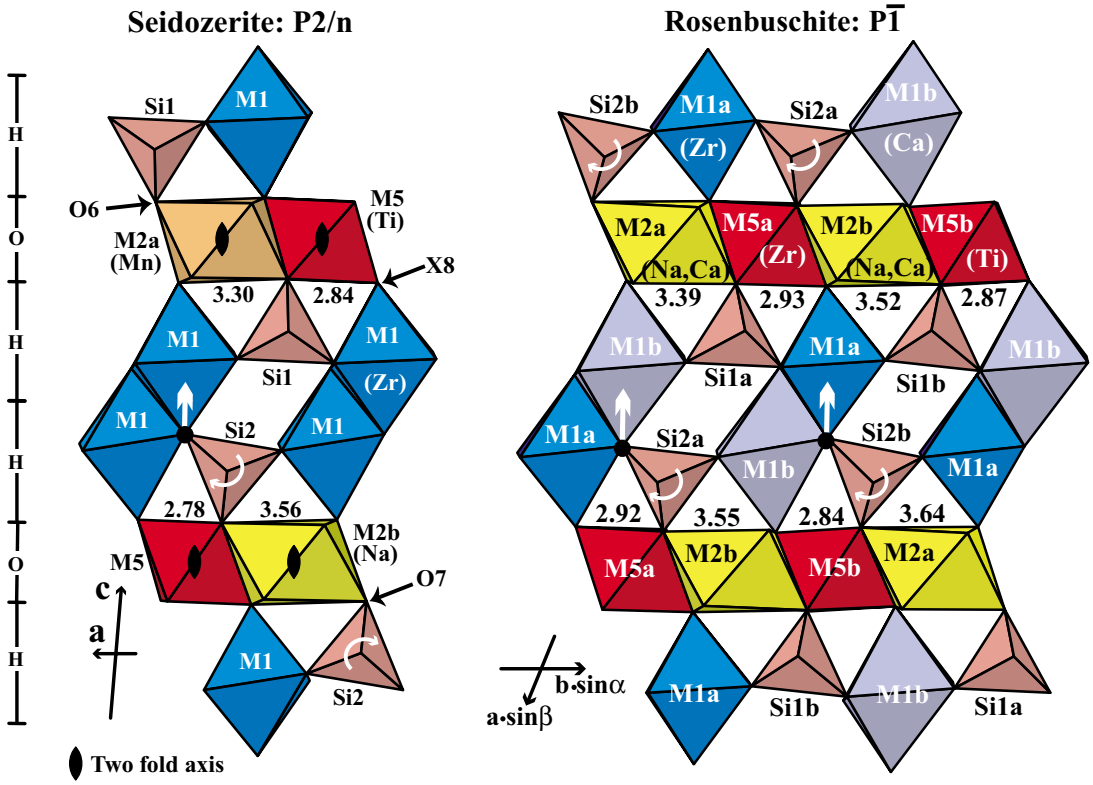

FIG. 13. Part of the structures of seidozerite and rosenbuschite showing the relationship among the sizes of the *M*2 octahedra, rotations of the Si tetrahedra and the attachment of tetrahedra to the adjacent *H* layer. The *O*3 positions are indicated by a black circle. The *H* and *O* layers are indicated to the left. The distances between *X*8 and the tetrahedron vertices common to the *O* layer are given in Å.

HOH-layers are in opposite directions relative to the central *HOH*-layer, resulting in the triclinic mode of stacking.

In the triclinic structures, the difference in the rotations of the tetrahedra is not as distinct as in seidozerite. In the variants of the rosenbuschite structure, the Zr–Ca order at the *M*1 sites also has a significant effect upon these rotations (Fig. 13). The *Si*1a tetrahedron has a low degree of rotation (2.97°), the *Si*2a and *Si*1b tetrahedra are rotated 6.21–6.43°, and the *Si*2b tetrahedron has a high degree of rotation (11.27°). With respect of the *Si*1a and *Si*2a tetrahedra, their edges facing the *M*5 octahedron are also connected to the relatively small *M*1a octahedron, whereas the corresponding edges of *Si*1b and *Si*2b are connected to the larger *M*1b octahedron. The combination of one small *M*5 and one large *M*1b octahedron joined to the same tetrahedron-edge favors a higher degree of rotation of the tetrahedron, when compared to the case with the small *M*1a octahedron joined to the same tetrahedron-edge as the *M*5 octahedron. Furthermore, the *O*3b corner of the *Si*2b tetrahedron is pulled toward the small *M*1a octahedron of the immediately adjacent *H*-layer, resulting in the largest rotation of the tetrahedra.

Conclusions:

1) Götzenite, hainite, kochite, rosenbuschite and seidozerite are based on the same fundamental structure, and they are considered members of the rosenbuschite group.

2) All members are triclinic, with space group $P\bar{1}$, except for seidozerite, which has monoclinic symmetry $P2/n$. Seidozerite is a configurational polytype to the other members of the group.

3) In this work, five different members of the group have been established. The general formula for the group can be represented by $(M1)_4(M2)_4(M3)_4(M4)_2(M5)_2(Si_2O_7)_4F_4X_4$. Götzenite and hainite have unit cells half the size of those of rosenbuschite and seidozerite, and their general formulae are accordingly halved. Simplified formulas for each member, following the scheme, are:

Götzenite: $Ca_2(Ca,Na)_2Ca_2NaTi(Si_2O_7)_2F_2F_2$

Hainite: $(Ca,Zr,Y)_2(Na,Ca)_2Ca_2NaTi(Si_2O_7)_2F_2F_2$

Kochite:
$Zr_2(Mn,Zr)_2(Na,Ca)_4Ca_4Na_2Ti_2(Si_2O_7)_4F_4O_4$

Rosenbuschite:
$Zr_2Ca_2(Na,Ca)_4Ca_4Na_2ZrTi(Si_2O_7)_4F_4O_4$

Seidozerite: $Zr_4Na_2Mn_2Na_4Na_2Ti_2(Si_2O_7)_4F_4O_4$

4) The *M*1 site hosts a variety of cations of different crystal-chemical properties: Ca, Zr, Mn and Y. The octahedron assumes different dimensions in order to accommodate these cations. This flexibility has a significant effect upon the size and deformation of the adjacent polyhedra and Si_2O_7 groups: a) The size of the *M*5 octahedron does not vary much, but the *M*5a octahedron connected to the Zr-dominated *M*1a octahedra differs from *M*5b in that it may contain significant amount of Zr. The *M*5a octahedron is slightly larger than *M*5b and has a higher O:F ratio in the *X*8 sites. b) The Si_2O_7 groups show three modes of bending, depending on the size of the two *M*1 octahedra. c) The degree of bending relates directly to a stretching of the *M*3 and *M*4 polyhedra, and also to the interatomic distance between these cations and *O*1. In the rosenbuschite variant of the structure, the *M*3 site, with the shortest distance to *O*1, contains significant amount of Na (25%). *M*4 is invariably within bonding distance to *O*1 and dominated by Na.

5) The column of *M*2 octahedra hosts Na and Ca only in the triclinic structure-type. In the monoclinic seidozerite, a smaller Mn octahedron is incorporated into this column, resulting in its shorter periodicity.

6) Our data indicate that Ca and Zr in the *M*1 position are only partially replacable. Chemical data suggest a solid-solution series between götzenite and rosenbuschite, and a compositional gap between rosenbuschite and seidozerite. Such a gap between rosenbuschite and seidozerite is explained by a dimensional misfit between the two structures, which cannot be compensated. This misfit results from differently sized octahedra and different mode of stacking of *HOH* layers. The Ca ↔ Zr replacement in the götzenite–rosenbuschite compositional series is compensated by adjusting the shape of the surrounding octahedra.

7) Zirconium may both replace Ca in the *M*1a site and substitute for Ti in *M*5a. This results in two compositional series. One series occurs between götzenite and kochite, in which Zr replaces Ca, and another between kochite and rosenbuschite, in which Zr substitutes for Ti. The Zr ↔ Ti substitution is only observed in the *M*5a position in those specimens in which Zr dominates at the *M*1a site.

8) The two modes of stacking of *HOH* layers in the configurational polytypes are related to the sizes of the *M*2 octahedra and the occupancy of the *M*1 positions. The monoclinic polytype is favored by two differently sized *M*2 octahedra and domination of Zr in the *M*1 sites, whereas the triclinic polytype is correlated with equally sized *M*2 octahedra and full or partial occupancy of Ca at the *M*1 sites.

Acknowledgements

We are indebted to: R.A. Gault, Canadian Museum of Nature, for his electron-microprobe analyses of the

specimens investigated, T. Balić-Žunić, University of Copenhagen, for his assistance during collection of single-crystal-diffractometry data, J.D. Grice, Canadian Museum of Nature, for fruitful discussions during the work, Alf Olav Larsen, who generously provided numerous specimens of the rosenbuschite group of minerals from the Langesund Fjord area, Norway, and to Dan Holtstam, the Museum of Natural History in Stockholm, who kindly provided the type material of rosenbuschite. We also thank the referees G. Ferraris and E. Sokolova for their helpful comments about the manuscript. The work was supported by the Danish Natural Science Research Council.

References

ATENCIO, D., COUTINHO, J.M.V., ULBRICH, M.N.C., VLACH, S.R.F.., RASTSVETAEVA, R.K. & PUSHCHAROVSKY, D.YU. (1999): Hainite from Poços de Caldas, Minas Gerais, Brazil. *Can. Mineral.* **37**, 91-98.

BALIĆ-ŽUNIĆ, T. & VICKOVIC, K. (1996): IVTON, a program for the calculation of geometrical aspects of crystal structures and some crystal chemical applications. *J. Appl. Crystallogr.* **29**, 305-306.

BETTI, F. (1998): Cristallochimica di silicati con formula generale $X_{16}(Si_2O_7)_4(O,OH,F)_8$. Master's thesis, Università degli Studi di Pisa, Pisa, Italy.

BLUMRICH, J. (1893): Die Phonolithe des Friedländer Bexirkes in Nordböhmen. *Tschermaks Mineral. Petrogr. Mitt.* **13**, 465-495.

BRESE, N.E. & O'KEEFFE, M. (1991): Bond-valence parameters for solids. *Acta Crystallogr.* **B47**, 192-197.

BRÖGGER, W.C. (1887): Forelöbig meddelelse om mineralerne på de sydnorske augit- og nefelinsyeniters grovkornige gange. *Geol. Fören. Stockholm Förh.* **109**, 247-274.

_____ (1889): Vorläufige Mittheilung über die Mineralien der grobkörnigen gänge der Südnorwegischen Augit- und Nephelinsyenite. *Z. Kristallogr. Mineral.* **15**, 103-104.

_____ (1890): Die Mineralen der Syenitpegmatitgänge der Südnorwegischen Augit- und Nephelinsyenite. *Z. Kristallogr. Mineral.* **16**.

BULAKH, A.G. & KAPUSTIN, YU.L. (1973): Götzenite from the alkaline rocks of the Tur'yev Peninsula, Kola Peninsula. *Zap. Vses. Mineral. Obschhest.* **102**(4), 464-466.

CANNILLO, E., MAZZI, F. & ROSSI, G. (1972): Crystal structure of götzenite. *Sov. Phys. Crystallogr.* **16**, 1026-1030.

CHRISTIANSEN, C.C., GAULT, R.A., GRICE, J.D. & JOHNSEN, O. (2003): Kochite, a new member of the rosenbuschite group from the Werner Bjerge alkaline complex, East Greenland. *Eur. J. Mineral.* **15**, 551-554.

_____, MAKOVICKY, E. & JOHNSEN, O. (1999): Homology and typism in heterophyllosilicates: an alternative approach. *Neues Jahrb. Mineral., Abh.* **175**, 153-189.

_____ & RØNSBO, J.G. (2000): On the structural relationship between götzenite and rinkite. *Neues Jahrb. Mineral., Monatsh.*, 496-506.

CUNDARI, A. & FERGUSON, A.J. (1994): Appraisal of the new occurrence of $götzenite_{ss}$, khibinskite and apophyllite in kalsilite-bearing lavas from San Venanzo and Cupaello (Umbria), Italy. *Lithos* **31**, 155-161.

EGOROV-TISMENKO, YU.K. & SOKOLOVA, E.V. (1990): Structural mineralogy of the homologous series seidozerite–nacaphite. *Mineral. Zh.* **12**(4), 40-49 (in Russ.).

FERRARIS, G. (1997): Polysomatism as a tool for correlating properties and structure. *In* Modular Aspects of Minerals (S. Merlino, ed.). *Eur. Mineral. Union, Notes in Mineralogy* **1**, 275-295.

_____, IVALDI, G., KHOMYAKOV, A. P., SOBOLEVA, S. V., BELLUSO, E. & PAVESE, A. (1996): Nafertisite, a layer titanosilicate member of a polysomatic series including mica. *Eur. J. Mineral.* **8**, 241-249.

JOHAN, Z. & ČECH, Z. (1989): New data on hainite, $Na_2Ca_4[(Ti,Zr,Mn,Fe,Nb,Ta)_{1.5}\square_{0.5}](Si_2O_7)_2F_4$ and its crystal chemical relationship with götzenite, $Na_2Ca_5Ti(Si_2O_7)_2F_4$. *C.R. Acad. Sci. Paris* **308**(II), 1237-1242.

MAKOVICKY, E. (1997): Modularity – different types and approaches. *In* Modular Aspects of Minerals (S. Merlino, ed.). *Eur. Mineral. Union, Notes in Mineralogy* **1**, 315-343.

_____ & BALIĆ-ŽUNIĆ, T. (1998): New measure for distortion for coordination polyhedra. *Acta Crystallogr.* **B54**, 766-773.

MELLINI, M. (1981): Refinement of the crystal structure of låvenite. *Tschermaks Mineral. Petrogr. Mitt.* **28**, 99-112.

MEN'SHIKOV, YU.P., PAKHOMOVSKY, YA.A & YAKOVENCHUK, V.N. (1999): Rosenbuschite from the Khibiny alkaline massif. *Zap. Vser. Mineral. Obshchest.* **128**(1), 63-68.

NEUMANN, H. (1962): Rosenbuschite and its relation to götzenite. *Norsk Geol. Tidsskr.* **42**, 179-186.

PEACOCK, M.A. (1937): On rosenbuschite. *Norsk Geol. Tidsskr.* **17**, 17-30.

PERCHIAZZI, N., MCDONALD, A.M., GAULT, R.A., JOHNSEN, O. & MERLINO, S. (2000): The crystal structure of normandite and its crystal-chemical relationships with låvenite. *Can. Mineral.* **38**, 641-648.

PUSHCHAROVSKII, D.YU., PASERO, M., MERLINO, S., VLADYKIN, N.D., ZUBKOVA, N.V. & GOBECHIYA, E.R. (2002): Crystal structure of zirconium-rich seidozerite. *Crystallogr. Rep.* **47**(2), 196-200.

RASTSVETAEVA, R.K., PUSHCHAROVSKII, D.YU. & ATENCIO, D. (1995): Crystal structure of giannetite. *Crystallogr. Rep.* **40**, 574-578.

SAHAMA, T.G. & HYTÖNEN, M.A. (1957): Götzenite and combeite, two new silicates from the Belgian Congo. *Mineral. Mag.* **238**, 503-510.

_____, SAARI, E. & HYTÖNEN, M.A. (1966): Relationship between götzenite and rosenbuschite. *Bull. Comm. Géol. Finlande* **222**, 135-144.

SEMENOV, E.I., KAZAKOVA, M.E. & SIMONOV, V.I. (1958): A new zirconium mineral, seidozerite, and other minerals of the wöhlerite group in alkaline pegmatites. *Zap. Vses. Mineral. Obschest.* **87**, 590-597 (in Russ.).

SHANNON, R.D. (1976): Revised effective ionic radii and systematic studies of interatomic distances in halides and chalcogenides. *Acta Crystallogr.* **A32**, 751-767.

SHARYGIN, V.V., STOPPA, F. & KOLESOV, B.A. (1996): Zr–Ti disilicates from the Pian di Celle volcano, Umbria, Italy. *Eur. J. Mineral.* **8**, 1199-1212.

SHIBAEVA, R.P., SIMONOV, V.I. & BELOV, N.V. (1964): Crystal structure of the Ca, Na, Zr, Ti silicate rosenbuschite, $Ca_{3.5}Na_{2.5}Zr(Ti,Mn,Nb)\ [Si_2O_7]_2F_2O(F,O)$. *Sov. Phys. Crystallogr.* **8**, 406-413.

SIMONOV, V.I. & BELOV, N.V. (1960): The determination of the structure of seidozerite. *Sov. Phys. Crystallogr.* **4**, 146-157.

SKSZAT, S.M. & SIMONOV, V.I. (1966): The structure of calcium seidozerite. *Sov. Phys. Crystallogr.* **10**, 505-508.

ZACHARIASEN, W.H. (1930): The chemical formula of the zircon pyroxenes and the zircon pectolite. *Norsk Geol. Tidsskr.* **11**, 216-218.

Received August 4, 2002, revised manuscript accepted August 27, 2003.